CHALMERS
UNIVERSITY OF TECHNOLOGY

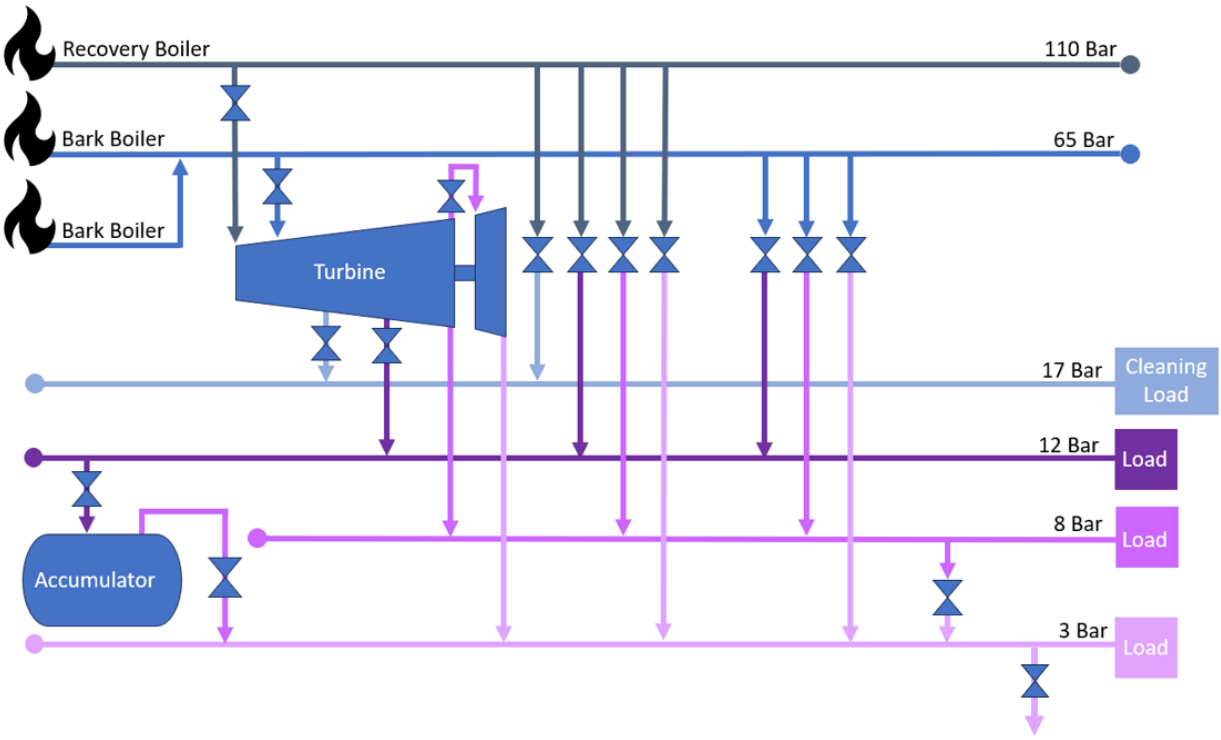

Modelling and Evaluation of Steam Net Control in a Pulp Mill

Master's Thesis in Sustainable Energy Systems

Monika Arvidsson & Agnes Lindgren

DEPARTMENT OF ELECTRICAL ENGINEERING
CHALMERS UNIVERSITY OF TECHNOLOGY
Gothenburg, Sweden 2024
www.chalmers.se

Master's thesis 2024

Modelling and Evaluation of Steam Net Control in a Pulp Mill

MONIKA ARVIDSSON
AGNES LINDGREN

CHALMERS
UNIVERSITY OF TECHNOLOGY

Department of Electrical Engineering
Division of Systems and Control
Chalmers University of Technology
Gothenburg, Sweden 2024

Modelling and Evaluation of Steam Net Control in a Pulp Mill

MONIKA ARVIDSSON
AGNES LINDGREN

Supervisor: Veronica Olesen, Electrical Engineering.
Supervisor: Eskil Svensson, Solvina AB.
Examiner: Torsten Wik, Electrical Engineering.

Master's Thesis 2024
Department of Electrical Engineering
Division of Systems and Control
Chalmers University of Technology
SE-412 96 Gothenburg
Telephone +46 31 772 1000

Cover: Illustration of the studied steam net system for an existing pulp mill.

Typeset in LaTeX
Printed by Chalmers Reproservice
Gothenburg, Sweden 2024

Modelling and Evaluation of Steam Net Control in a Pulp Mill
MONIKA ARVIDSSON & AGNES LINDGREN
Department of Electrical Engineering
Chalmers University of Technology

Abstract

In this thesis, modified control strategies are implemented in a simulation environment to evaluate the performance of a steam system in an existing pulp mill. The steam system consists of several pressure headers which are connected to multiple valves. In the existing control system, one controller aims to maintain a pressure set point for each pressure header. A smart split-range strategy, developed by Solvina AB, is used to distribute the signal from a given controller to valves that alter their opening degree according to the control signal. The aim of the presented work was to identify new solutions that change the control of the valves and the control hierarchy of the system to increase energy efficiency while maintaining or improving the system stability. Three different solutions were implemented in the software Dymola. The first solution deals with the opening sequence of non-linear valves. The second and third implementations consider the control sequence of steam excess at a pressure header and the control of the existing accumulator. To evaluate the performance, the steam system was tested by being exposed to three dynamic changes. These changes were a load trip, a load start-up and a partial turbine trip. It was found that there is a trade-off between decreased fuel usage and increased electricity generation. Furthermore, it was seen in some of the simulations that an improved accumulator usage could be achieved, but at the expense of decreased pressure stability, and vice versa.

Keywords: Energy Efficiency, Steam Net Control, Split-Range, Control System, Steam Network, Pulp Mill Process, Automatic Control.

Acknowledgements

We would like to thank Eskil Svensson, our supervisor at Solvina AB, for being supportive and patient with us. Also, we would like to thank our supervisor at Chalmers, Veronica Olesen, for giving good feedback throughout the project and helping us to understand the steam net control. Thank you Torsten Wik for being our examiner and showing your interest in the subject. Thanks to all colleagues at Solvina AB for the interesting discussions and for being so inclusive. Lastly, many thanks to our friend Jennifer Underdal. Without you, we would not have been writing this master's thesis together.

Monika Arvidsson & Agnes Lindgren, Gothenburg, May 2024

List of Acronyms

Below is the list of acronyms that have been used throughout this thesis listed in alphabetical order:

HL	High Limit
HP	High Pressure
IP	Intermediate Pressure
LC	Limit Control
LL	Low Limit
LP	Low Pressure
MC	Main Control
V	Valve

Nomenclature

Below is the nomenclature of variables that have been used throughout this thesis.

Variables

e	Error $(r - y)$
F	Controller
F_F	Feed Forward
G	Process
G_v	Disturbance
h	Enthalpy
IAE	Integrated Absolute Error
K_d	Derivative Constant
K_i	Integral Constant
K_p	Proportional Constant
LHV	Lower Heating Value
P	Power
Q	Internal Energy
$RMSE$	Root Mean Square Error
r	Set Point
T_i	Integral Time
T_d	Derivative Time
u	Controller Output
v	Disturbance Signal
y	Process Value

Contents

1

Introduction

This thesis is, in cooperation with Solvina AB, focusing on control strategies for the steam net at the pulp and paperboard mill Iggesund, situated in Sweden. Solvina AB is an energy consulting firm with expertise in the control of steam and power production [1]. Among other things, Solvina AB has developed an automatic control of the steam net system in Iggesund. However, it has been discovered that the automatic control still has potential for improvements, which gave rise to this thesis. New control strategies have therefore been proposed and evaluated in this thesis using the modelling program Dymola.

1.1 Background

Several pulp and paperboard mills exist in Sweden [2]. The process requires heat at different temperatures, which is provided by a steam net consisting of several pressure levels. For example, steam is used in the drying process of pulp and paperboard. In a steam net system, highly pressurised steam is generated in boilers and flows through reduction valves to provide steam at lower pressure levels. Each pressure level is represented by a so-called header that is connected to pipes where steam either enters or leaves.

One issue with steam net systems is their dynamic characteristics. Although the process is aiming for a constant steam demand, uncontrolled disturbances occur, causing fluctuations in the requested amount of steam. These disturbances could, for example, be tripping of a turbine or a machine in the pulp process, i.e., an undesired unplanned stop. Since boilers produce steam at a steady rate and are sensitive to rapid changes, the steam produced cannot always meet drastic reductions in steam requirements. As a consequence, a surplus of steam may be generated that is sent out to the atmosphere without being used in the process. This decreases the overall energy efficiency of the system and use of more fuel than necessary.

Another issue is the dependency on fossil fuels in the system. To achieve net zero carbon dioxide emissions in 2050, a reduction in fossil fuel emissions is needed [3]. Regarding the pulp industry in Iggesund, oil is used mainly to compensate for unexpected disturbances. Oil burners are advantageous compared to burners using black liquor or bark, in terms of response time to load variations. However, if the automatic control stability is improved, the oil usage can potentially be decreased.

1.2 Aim

This thesis aims to identify improvements of the current control system for a steam net system in a pulp mill, to increase the energy efficiency. This is defined in terms of reducing the amount of steam released to the atmosphere, minimising the input of oil fuel, and maximising electricity generation. To achieve increased energy efficiency, an investigation of how reduction valves can be controlled efficiently and how accumulator usage can be maximised is considered. Additionally, the stability of the current system must be maintained or improved. The research questions that will be answered are the following:

- How can the control of the reduction valves be modified?
- How can the control hierarchy be developed to use the accumulator more efficiently?

1.3 Limitations

Evaluations are limited to simulations in a virtual environment in Dymola and thus implementations in the real system are outside the scope. The work is limited to analysing the control system of the steam net. Other solutions, such as changing fuel type to reduce oil usage or changing components within the system, are not investigated. The project does not cover any economic evaluation of the implementations such as the cost of updating the automatic control system, cost of fuel or produced power.

2

Theory

This section first includes how energy efficiency can be evaluated in a process. Secondly, an overview of the pulping process and its steam system is given, as well as a theoretical background of the components that are used to produce and provide steam. Thirdly, control quality in a dynamic system is defined. Lastly, the theory behind the implemented automatic control in the Dymola model, including controllers and function blocks, is introduced and explained.

2.1 Energy Efficiency

Heat is a transfer of energy, causing an object to increase or decrease its temperature [4]. The driving force for this phenomenon to occur is temperature difference, where a large temperature difference causes a large heat flux. This heat flux may be accumulated as internal energy according to

$$Q = m \cdot \Delta h, \tag{2.1}$$

where the internal energy Q is calculated using the mass m and the enthalpy difference Δh between the system and its surroundings.

The performance of a process can be measured by calculating the energy utilisation factor (EUF) defined by

$$EUF = \frac{P_{el} \cdot t + Q_u}{Q_{fuel}}, \tag{2.2}$$

where P_{el} is the produced electricity over time t and Q_u denotes the energy used within the process [5]. Q_{fuel} is the internal energy of the fuel that is used to provide heat in the process and is defined by

$$Q_{fuel} = m_{fuel} \cdot LHV, \tag{2.3}$$

where m_{fuel} is the mass of the fuel and LHV is the lower heating value of the fuel. This lower heating value is defined as the amount of heat produced when combusting a unit quantity of a fuel, which accounts for the energy required to vaporise the water content in the fuel [6].

2.2 Pulping Process

The first part of the process to produce pulp is to debark the wood and create wood chips [7]. Wood chips are mainly made of cellulose fibres that are bound together with lignin. Since only cellulose fibres are used in pulp, the lignin needs to be dissolved. To separate the components, a chemical kraft process is often used. The cellulose fibres are then separated from lignin by adding an alkaline solution, named white liquor, that is cooked together in a digester. To provide heat in the digester, steam is used. After several hours of cooking in the digester, the pulp is produced and the rest product, named black liquor, is separated. The produced pulp can be bleached if desired and dried if the paperboard manufacturing is not situated at the pulp mill. Several other separation processes exist such as mechanical processes and other chemical processes. However, the kraft process has advantages that other methods lack. For instance, long fibres are created, which increases the strength of the pulp. Furthermore, the kraft process can be used for several types of wood, it removes most of the lignin, and the chemicals used have a high recovery efficiency.

2.3 Boilers

Boilers are used in pulp mills to produce steam that provides heat to the process and generates electricity. Different types of boilers are used to combust different fuels. For example, recovery boilers contain burners that are fuelled with black liquor and oil, while bark boilers have burners that burn bark, which is a rest product of the debarked wood and oil burners. Oil burners have a shorter response time than recovery and bark burners, making them suitable to use when steam supply fluctuations occur.

Recovery boilers are preferably used in pulp mills with a kraft process since both steam is produced and chemicals are recovered [7]. The burner in a recovery boiler uses the rest product from the digester, i.e., black liquor containing lignin and other contaminants, as fuel. First, the concentration of black liquor is increased by heating the solution and evaporating the water. By removing the water, the black liquor achieves a higher energy content and becomes a more efficient fuel for the burner. The concentrated black liquor is then combusted in the boiler, and the inorganic chemicals form a molten smelt that is removed. This is further processed in a recausticizing process where chemicals are added to produce white liquor. The white liquor can then again be used in a digester to separate the cellulose fibres from lignin and produce pulp.

2.4 Steam Turbines

In steam turbines, steam is used to convert thermal energy to mechanical work [5]. This work can then be converted into electricity in an electrical generator that the steam turbine is connected to. A steam turbine consists of stator blades that accelerate the steam [8]. As the working fluid enters the turbine with high enthalpy and is accelerated throughout the turbine, the rotor blades will rotate and convert a part of the kinetic energy to mechanical work. Consequently, the steam enthalpy drops as the steam expands throughout the turbine. At the same time, the pressure drops from high pressure (HP) to low pressure (LP).

There are several types of steam turbines, as illustrated in Figure 2.1, including condensing steam turbines, back-pressure steam turbines, and extraction steam turbines [5]. In a condensing steam turbine, the exhaust saturated steam is condensed in a condenser at low pressure. Back-pressure steam turbines are characterised by a higher exit steam pressure where the exhaust steam is not saturated. Consequently, the exhaust steam can be used further in industrial processes requiring steam. At the same time, less electricity is generated than in a condensing steam turbine since the pressure drop is lower. Different back-pressure steam turbines generate various amounts of work depending on the designed back pressure. A higher back pressure results in a smaller enthalpy drop, and less produced power. Further, extraction steam turbines have outlets throughout the turbine to allow extraction of steam at intermediate pressure (IP) levels. Both condensing steam turbines and back-pressure steam turbines can be extraction steam turbines, as shown in Figure 2.1d and Figure 2.1b.

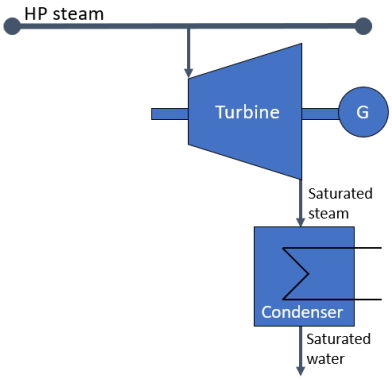

(a) Condensing turbine.

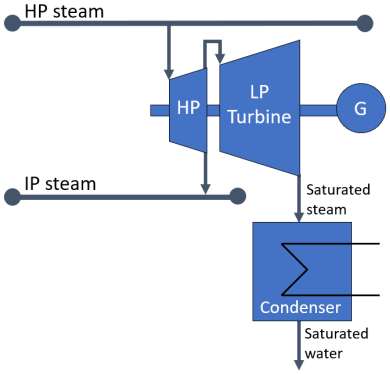

(b) Extracting condensing turbine.

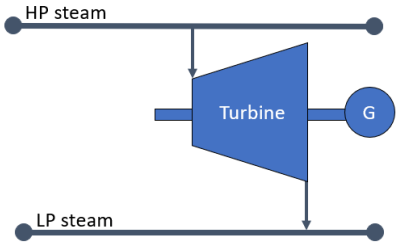

(c) Back-pressure turbine.

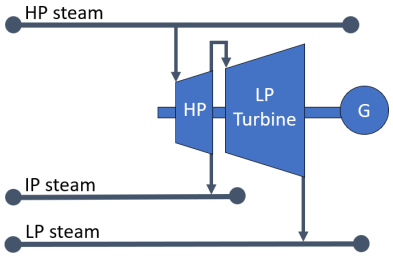

(d) Extracting back-pressure turbine.

Figure 2.1: An overview of different types of steam turbines.

2.5 Steam Accumulator

To compensate for variations in steam demand, i.e., disturbances, an accumulator can be added to a steam net system. An accumulator is a tank that stores steam when there is a surplus in the system and provide steam when there is a deficit. As seen in Figure 2.2, the accumulator contains a mixture of water in vapour phase and liquid phase. Highly pressurised steam is injected into the water, which causes the steam to condense. The enthalpy in the water then increases, as does the working pressure and temperature in the vessel. A pipe that is mounted into the accumulator allows the steam to exit at a lower or equal pressure level to the injected steam. If no steam is entering the accumulator while the steam outlet is open, the working pressure will instead decrease. Moreover, an accumulator is often provided with water inlet and water outlet to control the water level. Due to heat losses in the system, water will rise in the accumulator if the level is not controlled [9]. Furthermore, the capacity of the accumulator is limited by its size. The required size is inversely proportional to the difference in inlet and outlet pressure, and directly proportional to the working pressure.

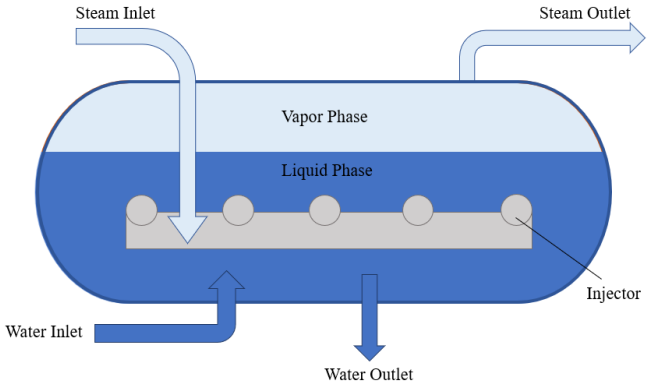

Figure 2.2: Visualisation of a steam accumulator containing steam and water.

2.6 Valves

Valves are connected in pipes to control the mass flow of a fluid, e.g., steam. By varying the opening degree of a valve, the mass flow through a pipe can be controlled. For control valves, the opening degree is a mechanical response of an actuator. Many types of valves exist with different designs, sizes, nominal pressure levels, and for different working fluids [10].

2.6.1 Types of Valves

Valves can be divided into three main groups according to their function: on-off valves, throttling valves and non-return valves [10]. On-off valves are either fully open or fully closed. One example of on-off valves is pressure-relief valves that fully open when a preset pressure level is exceeded. Moreover, throttling valves can in contrast to on-off valves have an opening degree ranging from 0% to 100% open. The opening degree is often controlled by an actuator, and the valve is then classified as a control valve. The third type of valve,

non-return valves, restricts the working fluid to only flow in one direction. This could be beneficial when no backflow is allowed even though a negative pressure drop occurs.

Another type of valve is reduction valves, also named desuperheater valves. The pressure and temperature of the superheated steam is then reduced by injecting water, e.g., with spray nozzles [11].

2.6.2 Valve Characteristics

Control valves are used to restrict the mass flow of a medium in a pipe, for instance a steam flow. The valve is normally connected to an actuator which controls whether the opening degree of the valve should remain or be changed. However, the opening degree of the valve does not always correspond linearly to the mass flow through the valve. Often, three design characteristics are considered: fast opening, linear, and equal percentage [12], as seen in Figure 2.3. A linear characteristic is preferable for the controller since its output signal then linearly corresponds to the mass flow in the valve, without any change of the controller parameters. Nonetheless, in some processes it can be beneficial to have a fast opening or equal percentage response, depending on the process profile [12].

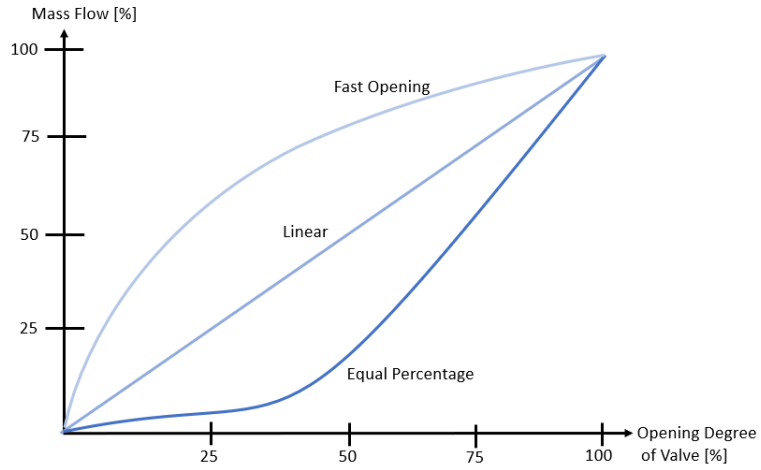

Figure 2.3: Graph showing three different valve characteristics.

It is not only the design of the valve that affects its response of a control signal but also, e.g., friction, hysteresis, and pressure drop. The friction force acts in opposition to the force of opening or closing the valve. Consequently, the actuator force needs to overcome the friction force in order to control the opening degree of the valve. If the friction force is larger or equal to the force from the actuator, the phenomenon hunting occurs where the valve is not moving although the actuator sends out a signal. Friction becomes a larger problem as the valve ages since they need to be tightened more by the gasket with usage to prevent leakage. Moreover, valve hysteresis indicates how much backlash that exists. The delay is normally caused by wear of the valve [12]. Furthermore, the mass flow through the valve varies with pressure drop, where an increased pressure drop results in an increased mass flow.

2.6.3 Linearisation

If a process is non-linear it can be compensated in the controller with gain scheduling, i.e., changing the controller constants depending on which interval that is regulated [12]. However, it is desirable to have a linear process to avoid gain scheduling as it can be difficult to do correctly. By linearising the process that e.g., contains non-linear valves, the controller will receive a linear response and thus gain scheduling can be avoided.

2.7 Valve Actuators

To convert the signal from a controller to a corresponding mechanical motion, actuators are used [13]. The actuator applies a force or a torque on a valve, which changes the degree of opening, resulting in a new mass flow through the valve. One important prerequisite to yield a precise operation is to attach the actuator securely and solidly to the body of the valve [13].

Energy is required for the actuator to transform signals into motion or force, and there are different types of actuators that can be used for this. Most commonly they actuate by electricity, pneumatics, or hydraulics which, respectively, use electrical energy, compressed air, and fluid power to drive the motion [14]. Depending on the actuator requirements for the process, such as response time, accuracy, durability, and reliability, the selection of type varies.

Figure 2.4 shows the basic principle of an actuator which uses an energy source to operate and receives a signal input from a controller. The actuator output is sent to a valve, i.e., the object that the actuator is supposed to control, and its degree of opening is altered. This valve output is then measured using a sensor and sent back to the controller, creating a feedback loop.

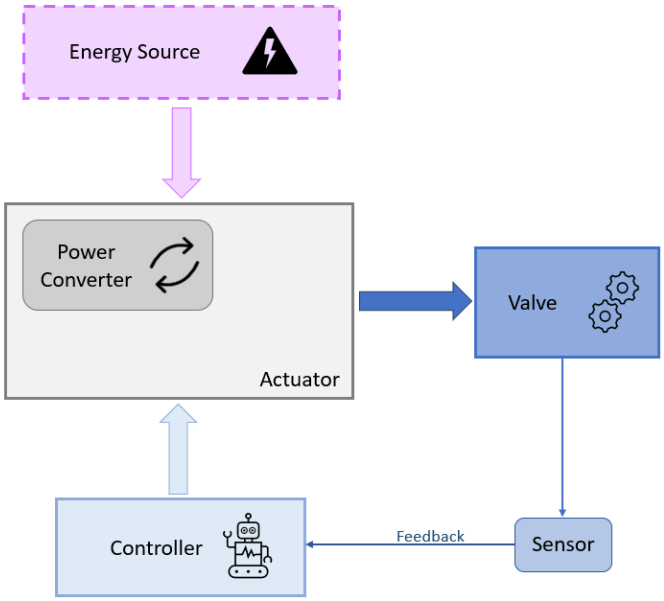

Figure 2.4: Basic working principle of an actuator with a feedback sensor.

2.8 Control Quality In a Dynamic System

Many processes are dynamic and to some extent unpredictable due to stochastic variations. An example of variation is transient disturbances that are caused by temporary changes within a system. Variations provoke fluctuations in process values and can vary in time and shape. Load changes can also cause fluctuations in the system and can be a result of production stops or varied requirements of heat in a process. By optimising the control quality, that is, striving towards stability, minimum deviation and duration, the effect of disturbances within the system can be minimised. System stability is defined as maintaining the process value within its limit, thus never growing uncontrollably or executing growing oscillations [15]. Moreover, minimum deviation ensures that the difference between the process value and the set point value is minimised, while minimum duration aims to minimise the time length of which a disturbance affects the controlled variable.

2.9 Feedback

To prevent undesired effects from disturbances and achieve high control quality, feedback can be used [16]. Figure 2.5 shows a feedback system with a controller F, a process G, and a disturbance G_V. The set point r is compared with the output of the process y, forming an error e. Based on this error, which ideally is zero, the controller adjusts the controller output u, also called the control signal, which enters the process that gives a new output of the process y. The process output is affected by some disturbance G_V, causing the error to increase. Disturbances can for instance be different process variations or noise. This principle to measure and calculate the error and adjust the controller output accordingly is named a feedback loop [16]. As a result, a more stable system which is less sensitive to process variations may be achieved.

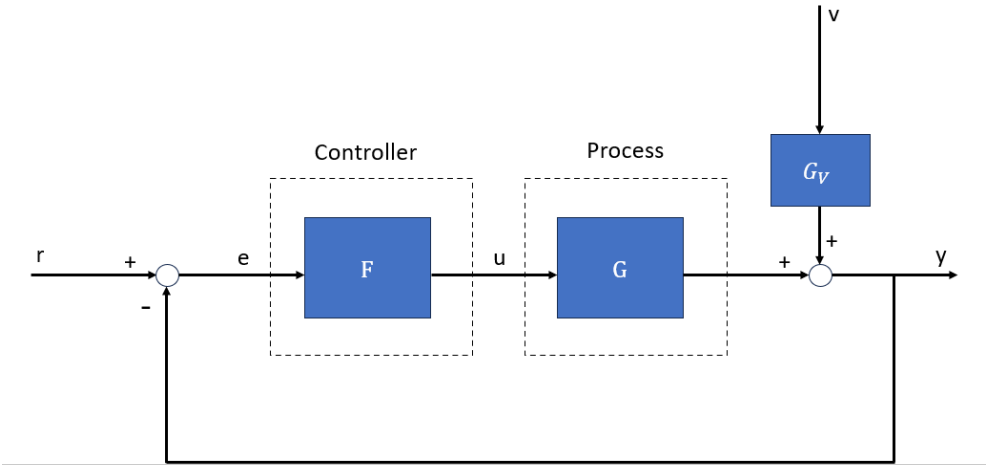

Figure 2.5: Block diagram of a process with a feedback controller.

2.10 PID - Controller

The PID-controller consists of three separate parts: a proportional, an integrating, and a derivative part [17]. The proportional part is a product of the error multiplied by a

constant K_p, forming a proportional gain. A high proportional constant leads to a high controller output, which results in a more aggressive tuning if deviation occurs. The following equation shows the calculation of the control variable using a P-controller.

$$u = K_p\,(r - y) + u_{offset} \tag{2.4}$$

The offset u_{offset} is the default control signal when the process is operating during normal conditions. However, this term is prone to yield a steady-state error. As a deviation in the process value occurs, the control signal adjusts accordingly to minimise the difference from the set point, i.e., reducing the error e. However, as the output approaches the set point, the control signal decreases leading to a residual error where the controller output never reaches the set point value.

By adding an integrator, as seen in

$$u(t) = K_p\,e(t) + K_i \int_0^t e(\tau)\,d\tau \tag{2.5}$$

this remaining error can fully diminish. The time dependent integral constant K_i is used to adjust the offset, and the integral of the error changes the controller variable as a result. The integral constant can be calculated according to

$$K_i = \frac{K_p}{T_i},$$

where T_i is the integral time. An additional term that can be added is the derivative part. This term has an anticipating ability, that is, it predicts what the output is expected to be in the future [17]. The output of a PID-controller is given by

$$u(t) = K_p\,e(t) + K_i \int_0^t e(\tau)\,d\tau + K_d\,\frac{d}{dt}\,e(t), \tag{2.6}$$

where the last term represents the derivative part. The derivative constant K_d is defined as

$$K_d = K_p \cdot T_d$$

where T_d is called the derivative time constant. Figure 2.6 shows a function block of a PID-controller where the error passes through the proportional, integrator, and derivative part before entering the process G.

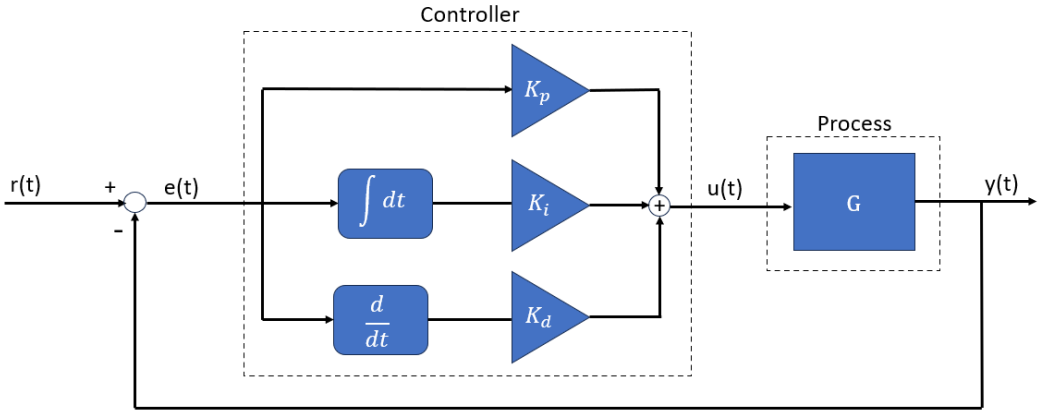

Figure 2.6: Block diagram with a PID-controller and feedback loop of the output signal $y(t)$.

2.11 Anti-Windup

A difficulty that may arise when using the integrator part in a controller is integrator windup [17]. Actuators have limitations, e.g., valves cannot withstand a larger opening degree than 100%, and if the control signal u exceeds the limit of the actuator, the valve cannot be controlled [16]. As a result, the actuator will not react to any control signal increase if it already has reached its limit u_{max}. If the set point is not reached despite having a controller output at its saturated value (u_{max}), the integrating part continues to increase due to the remaining error. Consequently, the calculated new desired control signal will continue to increase above u_{max}. Figure 2.7 shows an illustration of a process where the process value does not reach the new set point value. The control signal output u_{out} is equal to the desired control signal u as long as it does not exceed u_{max}. When u is greater than u_{max}, u_{out} is equal to u_{max}.

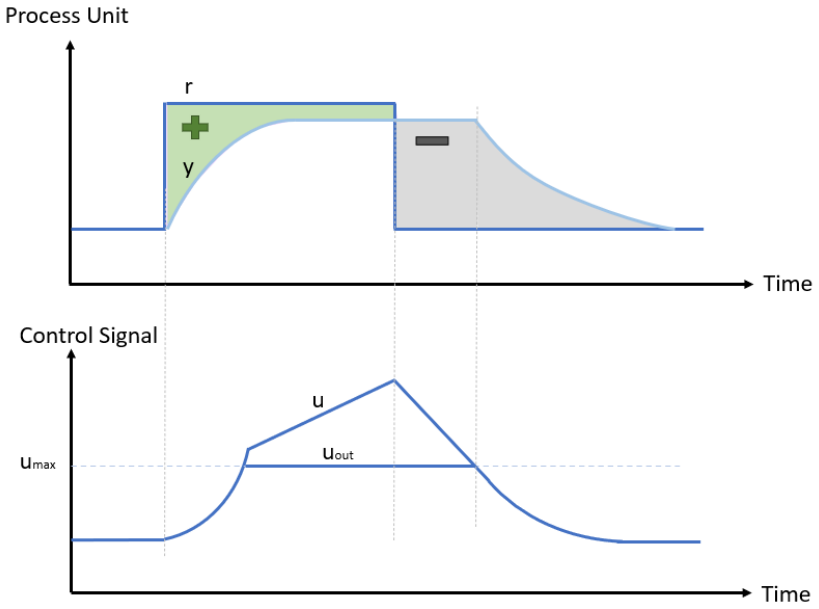

Figure 2.7: Integrator windup of a process y with set point changes r.

When the control signal u is above the actuator's limit u_{max}, the process value y may not react immediately if the set point r decreases. As the set point changes in Figure 2.7, the control error becomes negative and the control signal starts to decrease from its current value. However, since the control signal u has become larger than its limit, a delay is caused since u has to reduce its value before it can affect the process again, which prolongs the system response. By allowing the control signal to exceed its limit, windup is present. To avoid windup, it is necessary to stop the integration of the error when u reaches its saturated value u_{max}. This strategy is called anti-windup [17].

2.12 Feed Forward

As mentioned earlier, feedback is necessary to correct deviations that may occur within the process. One alternative to correct these deviations in advance is by implementing feed forward (F_F). By allowing the controller output to compensate for disturbances (G_V) that are expected to occur, the process is able to yield a smoother operation. Furthermore, by combining feed forward with feedback control, any error that the feed forward cannot fully compensate for is handled by the feedback. Figure 2.8 shows a combined feed forward and feedback system where F_F is added before entering the process G.

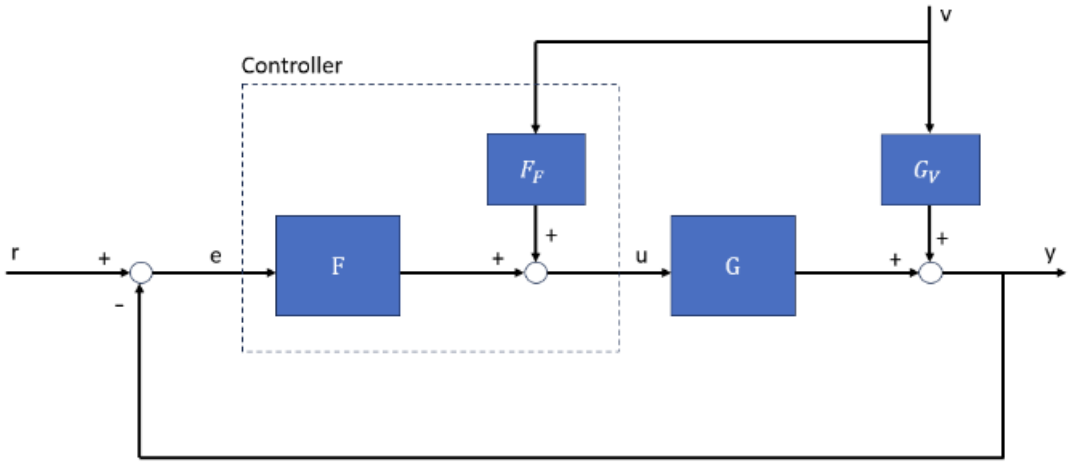

Figure 2.8: Example of a process with feedback and feed forward.

2.13 Split-Range

To provide control of several objects, such as valves, the split-range strategy can be used [17]. This strategy is useful if several objects are associated with one common control signal from a controller.

Figure 2.9a illustrates an example of three parallel valves of different sizes that are controlled by the same controller, and their corresponding operating ranges are shown in Figure 2.9b. It can be seen that the opening degree of valve V_1 is controlled when the controller output lies between 0% and 25%. As the controller output further increases, valve V_2 and valve V_3 start to open sequentially and V_1 remains locked at full opening.

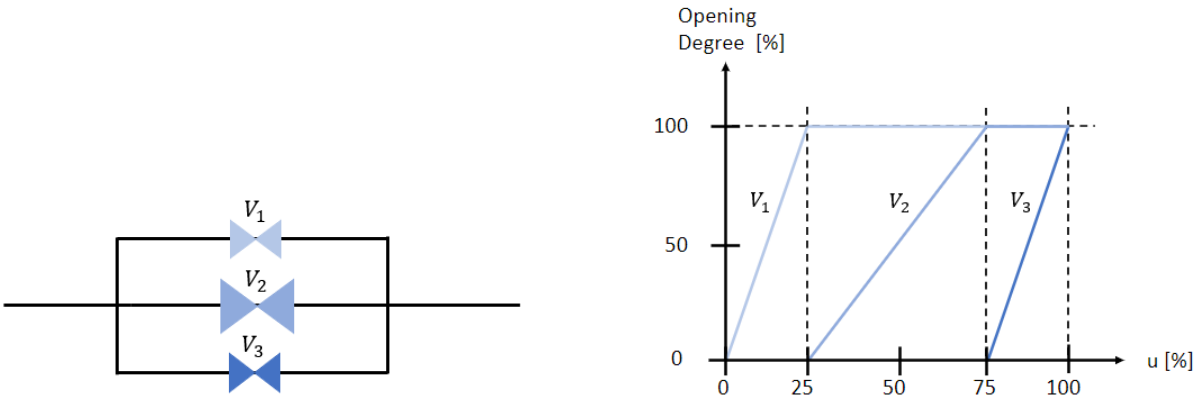

(a) Illustration of three valves with different sizes in a system.

(b) Split-range of the three valves.

Figure 2.9: Split-range strategy applied to three valves where the controller output is distributed among the objects.

Another way to illustrate the effect of the controller output over the three valves can be seen in Figure 2.10, where a controller output of 40% corresponds to valve 1 having an opening degree of 100% and an opening degree of 30% for valve 2. Since no control signal lies within the range between 75% and 100%, valve 3 remains closed.

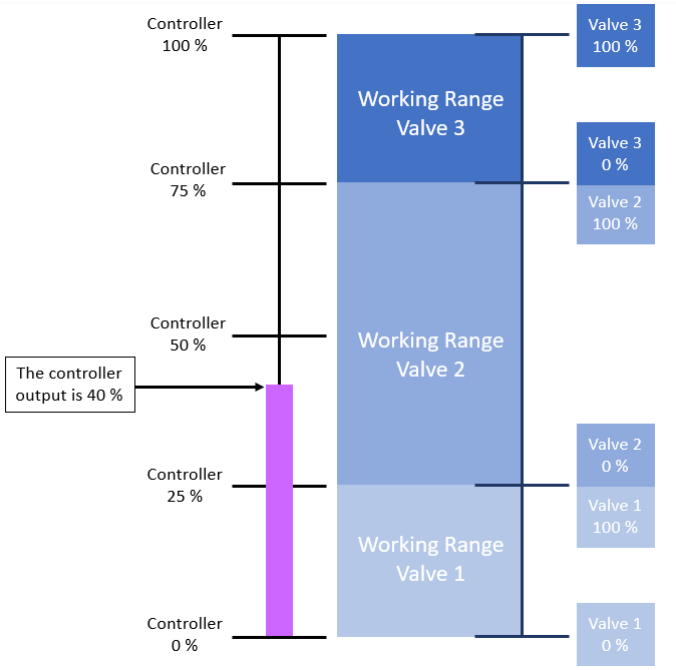

Figure 2.10: Illustration of the concept split-range. When the controller output is 40%, valve 1 opens 100%, valve 2 opens 30%, and valve 3 remains closed.

3

System Description

The studied steam net system in this project is shown in Figure 3.1. As seen, the system consists of six headers with unique pressure levels. Steam is first produced in boilers connected to the production nets 110 bar and 65 bar. A recovery boiler that is fuelled with black liquor in normal conditions and spiked with oil when more steam is needed, produces steam at 110 bar (HP1). Steam at 65 bar (HP2) is generated using two separate boilers, both including a bark burner and an oil boiler. The oil burners are used when the steam produced from bark is insufficient. The production nets are connected to the lower pressure nets with reduction valves, e.g., reduction valve 110/3 is found between the 110 bar header and the 3 bar header. As a reduction valve opens and steam streams, the pressure at the upstream header is reduced and the downstream header increases its pressure. Since the pressure levels at the headers can vary, so will the pressure drop in the reduction valves and thus the mass flow. In Figure 3.1, the valves are illustrated as one valve between each pressure level. This is a model simplification since the real steam net system has one to three valves installed in parallel. The 12 bar (IP1), 8 bar (IP2), and 3 bar (LP) headers are so-called consumer nets because they provide the pulp and paperboard process with steam. Steam on the 17 bar header is only used to clean the recovery boiler.

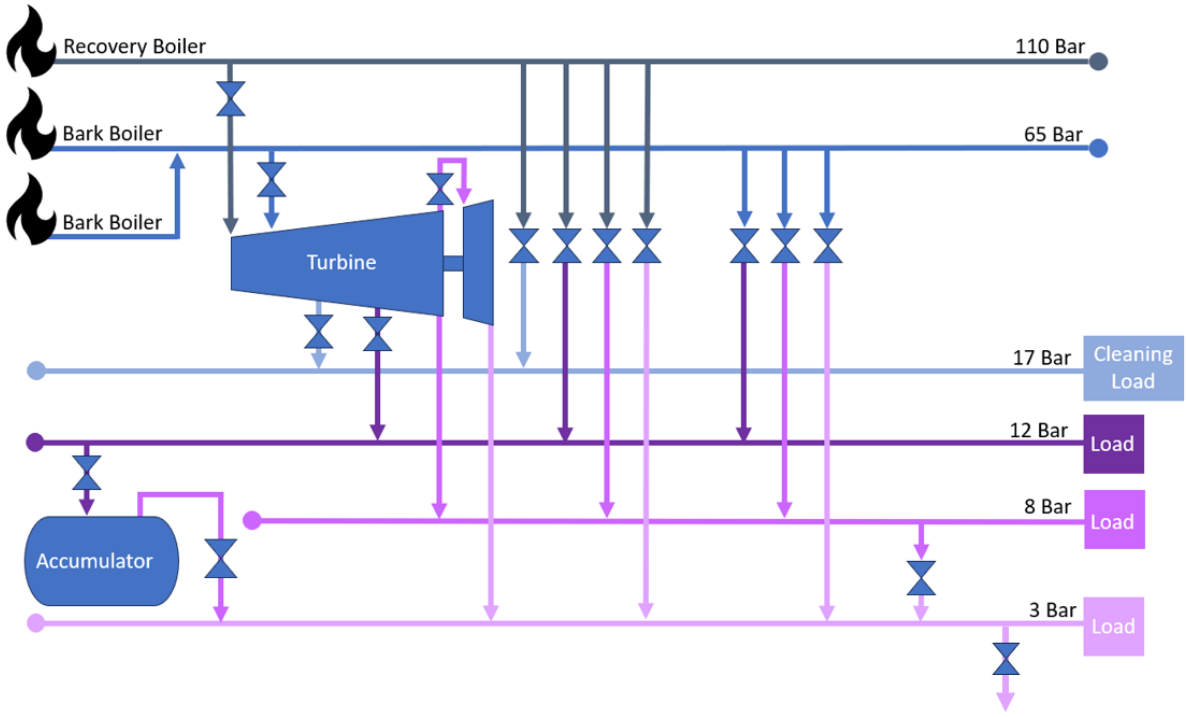

Figure 3.1: Simplified scheme of the steam net system at Iggesund. The cleaning load refers to the steam used to clean the recovery boiler, while the loads represent the process.

Moreover, the system in Figure 3.1 includes an extracting back-pressure turbine where electricity is generated. However, electricity generation is secondary to providing the process with steam. The generated electricity can both be used internally and sold to the grid when a surplus is produced. The inlet and outlet flows of the extracting back-pressure turbine are restricted by non-return valves, to prevent back flows in the turbine. Furthermore, a steam accumulator is connected between the 12 bar header and the 3 bar header. The accumulator aims to be filled when there is a surplus of steam in the system and in contrast, provides the 3 bar net with steam when it experiences a steam deficit. When the system has a larger surplus of steam, pressure relief valves are used on the 3 bar net. The pressure relief valves emit steam into the atmosphere and their usage is therefore classified as a loss in the system.

In addition to the components used in the system, a control system is used to obtain the desired pressure at each header. With a stable steam net, the heating requirements in the process will be satisfied, and thus the purpose of the net is achieved. The following sections include further information regarding the current automatic control of the system.

3.1 Main Control and Limit Control

The controller F uses split blocks to control objects, as seen in Figure 3.2. These split blocks can be restricted by a limit control (LC), that is, restricted by a high limit (HL) or a low limit (LL). This means that the opening degree of a valve does not necessarily have to be limited by the mechanical valve itself but by other limitations. For instance, a deficit of steam in one header may result in a fictional maximum opening degree being set, i.e.,

HL of a valve connected to the header to prevent the pressure from further decreasing. The split blocks consider the output y to be within the limits and the signal is sent to an actuator connected to the valve. The output signal of a header y is sent to the actuator and is said to possess a so-called main control (MC) over the valve, as it is controlling its opening degree. If LC restricts the valve from opening or closing to a desired point, any remaining signal u is sent to the next split block with the same working principle.

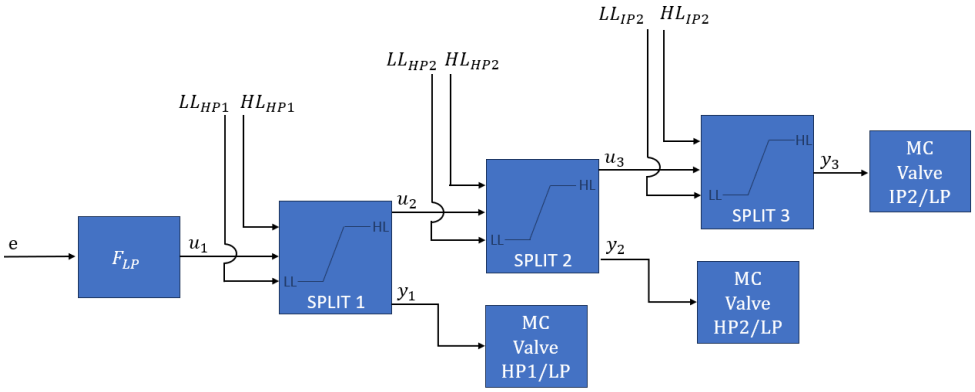

Figure 3.2: Example of split-range with HL and LL in each split block.

The example illustrated in Figure 3.2 considers the split-range for an LP controller that has MC over three valves. The incoming HL and LL to the splits are inputs from the HP1, HP2, and IP2 controllers respectively.

3.2 Header Controller

Each header has a main controller that aims to achieve the set point pressure level. The controller controls the mass flow inlet and outlet depending on whether there is a surplus or deficit of steam in the header. Figure 3.3 shows the split block order for the 110 bar controller. During normal conditions, the main controller uses the turbine inflow split block. If the amount of steam increases in the header, so does the control signal, causing the turbine inflow to increase. As a consequence, the pressure level should be reduced. However, if the header still experiences a steam surplus, the LL of reduction valves 110/3 will increase and force the valve to open. If, in contrast, the pressure level decreases in the 110 bar header, the control signal decreases resulting in a decrease of the turbine inflow. If the pressure level remains low, the control signal moves to the split block controlling the HL of the reduction valves 110/3. This will decrease the HL and force the valve to close. If a steam deficit still is present in the header, the 110/8 and 110/12 reduction valves will accordingly be forced to close due to their lowered high limits. The split block order for the other production net is presented in Figure 3.4, i.e., the split blocks for the 65 bar controller.

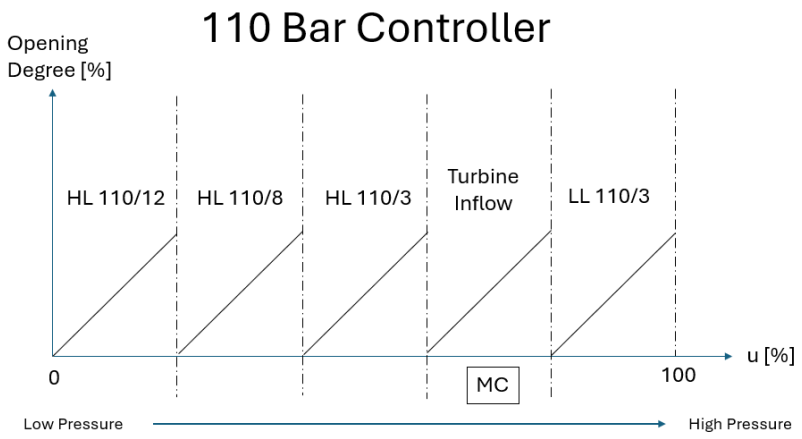

Figure 3.3: Split block order for the 110 bar controller.

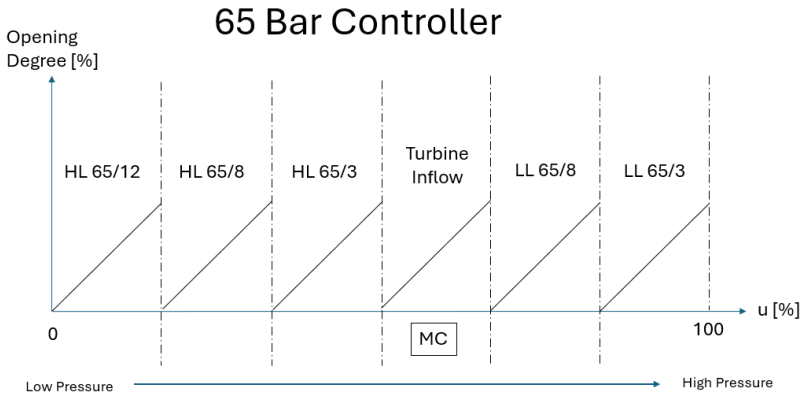

Figure 3.4: Split block order for the 65 bar controller.

To provide control of the different objects with the controller on each header, the controller must know the degree of freedom, that is, the total amount of mass flow that may be controlled in and out from each header. Each split block represents either an LC or MC over specific valves with different valve sizes. The size of these valves is summed up and multiplied with the control signal to achieve the control signal in mass flow units, which is distributed among the objects. Figure 3.5 visualises the conversion of the control signal where the signal that enters the split blocks is given in mass flow.

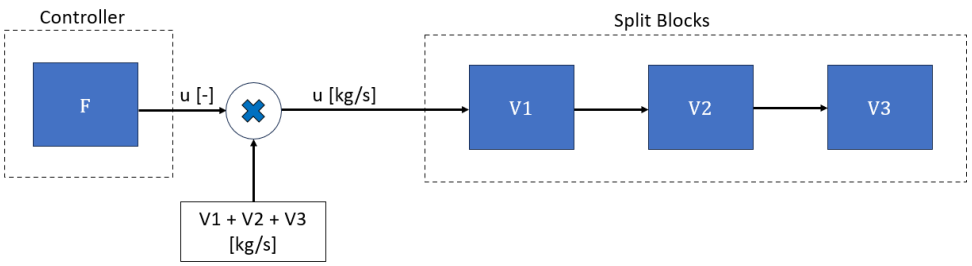

Figure 3.5: Illustration of a control signal conversion from a controller into mass flow units.

3.3 Smart Split-Range

As previously mentioned, external LL and HL in split blocks can be set from other pressure headers. This provides a hierarchical structure within the system. However, it can cause issues with deadbands within the control signal. An example is shown in Figure 3.6a where an external HL of 75% is set on valve 1. The controller signal is set to 100% which is equivalent to all the valves being fully open. However, due to the deadband, no regulation occurs at a control signal between 15% and 25% since valve 1 is restricted by its HL. Note that valve 2 starts to open when the control signal reaches 25%, despite the deadband. To prevent deadbands within the control signal, all high limits are moved to the upper part of the control signal, resulting in a maximum controller output of 90%, as shown in Figure 3.6b. Low limits will in contrast be moved downwards, determining a minimum value of the control signal. The implementation of smart split-range in the model is further presented in the two studies by Svensson [18] and Svensson [19].

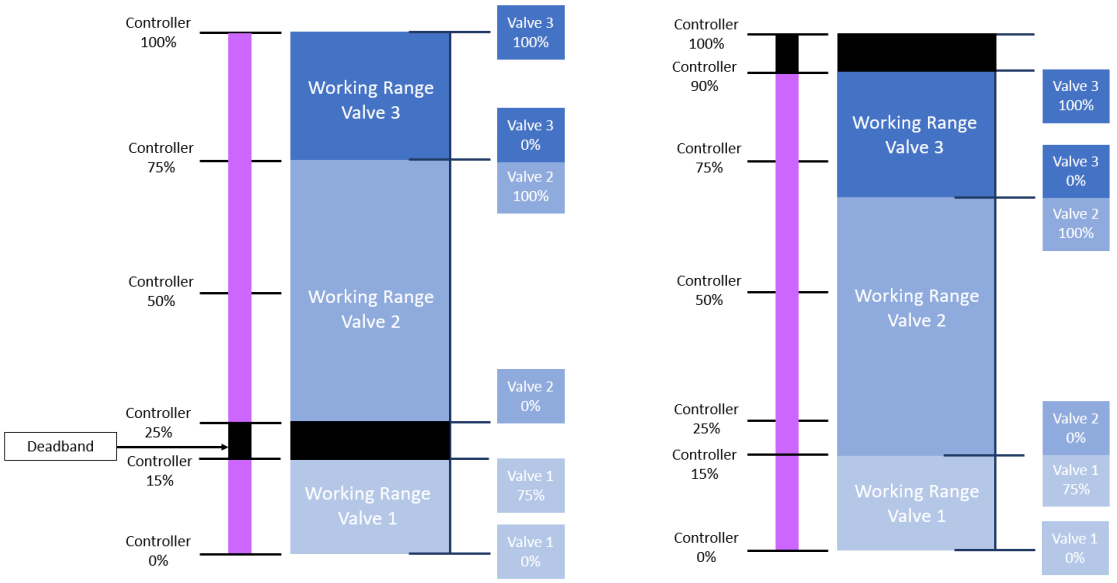

(a) A HL of 75% is set on valve 1 causing a deadband in the controller signal.

(b) The working ranges of the valves are moved downwards to prevent a deadband between valve 1 and valve 2.

Figure 3.6: Handling of deadband in the smart split-range.

3.4 Control Hierarchy

The headers are prioritised from high to low pressure since higher pressure levels provide lower pressure levels with steam, and vice versa is impossible. Thus, if the 110 bar header is tripping it affects the whole steam net system while a trip on the 3 bar net does not hinder any other header to be supplied with steam. This means that the 110 bar header has the highest priority to maintain its set point pressure level, as it is the highest pressure level in the system. If a higher pressure header has an excess of steam, steam will be sent down to the low pressure headers and the pressure relief valves that are connected to the 3 bar header are used as the last option to balance the system. However, the 17 bar header

is an exception since it is only used to clean the recovery boiler and therefore has its own independent control system.

To maintain a steam balance, valves are used to alter the inflow and outflow of steam between the headers, the turbine, and the accumulator. If one of the production headers experiences steam excess, the valves in the turbine inlet is first utilised to increase the electricity generation. If these valves are completely open and it is still not sufficient to balance the pressure level on that header, reduction valves are used. However, reduction valves are used at the bare minimum to avoid high pressurised steam being cooled down. From an energy perspective, it is undesirable to combust fuel to achieve a high temperature and pressure if steam is immediately cooled down.

3.5 Control of the Accumulator

The pressure inside the accumulator is desired to range between 3 and 12 bar. When 12 bar is reached, no flow into the accumulator is possible as no pressure difference is present. The same principle applies to the outlet valve when the accumulator pressure is 3 bar. Figure 3.7 shows an illustration of the main control of the inlet and outlet valves connected to the accumulator. The inlet valve into the accumulator is controlled from the 3 bar controller with limit control regulated by the 12 bar header. This limit control forces the valve to open if the pressure is too high on the 12 bar header and in contrast close when a low pressure occurs. The outlet valve from the accumulator is also controlled from the 3 bar header although without limit control since the flow through the valve only affects the 3 bar header itself.

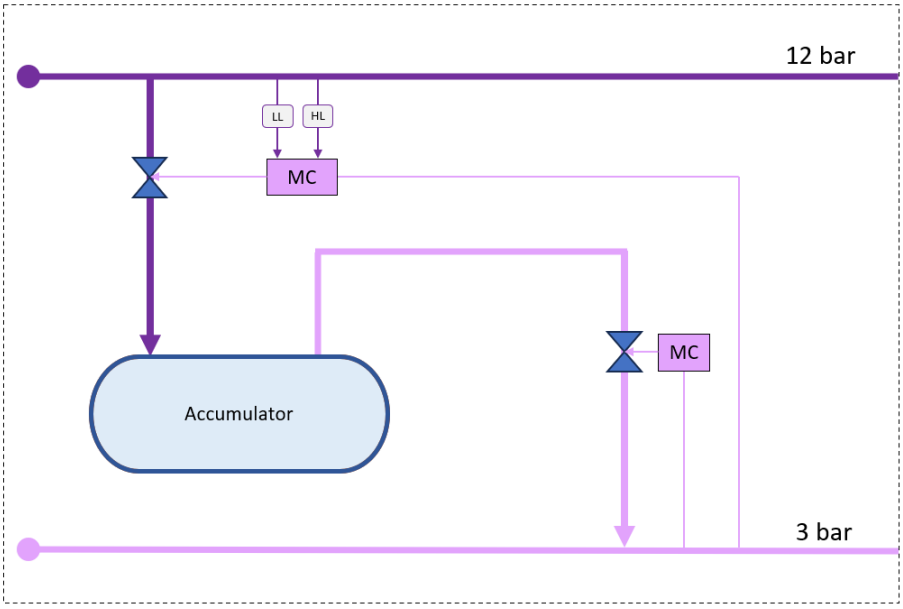

Figure 3.7: Illustration of the accumulator control with main control and limit control.

If the 3 bar header experiences a lack of steam, the outlet valve from the accumulator opens to provide more steam to flow to the 3 bar header. If the opposite occurs, the 3 bar header opens the accumulator inlet valve, causing the 12 bar header to experience a lack

of steam. As a consequence, the extraction valves from the turbine to the 12 bar header open more. This causes a reduction in the remaining steam flow from the turbine to the 3 bar header, which is the desired effect as the 3 bar header experienced steam surplus.

3.6 Control of the Boilers

The fuel supply in the burners is controlled by controllers with the accumulator pressure as process value. The accumulator pressure aims to reflect the balance between the supply and demand of steam in the system. Depending on the need for more steam, the fuel input in the burner can either increase or decrease. Oil burners respond quicker to pressure variations than bark burners and recovery burners, which is the reason why oil is mainly used during system fluctuations. If the accumulator pressure falls below a determined pressure level, oil burners are turned on. Although oil burners have a quicker response to fluctuations than bark and recovery burners, the response is still slow compared to how fast a fluctuation can occur in the steam net system.

4

Methods

The control system of the steam network was thoroughly analysed to acknowledge weaknesses that could be improved. From that, three potential improvements were selected and implemented in the Dymola model. By using the original model as a reference, comparisons were feasible to assess the impact of the implementations in the system.

Three different dynamic operating cases were selected to evaluate the implementations. These cases were added after the model was ensured to have reached steady state and the loads were at their default values. The first operating case selected included a load trip on the 3 bar header followed by a load start-up. A load trip is defined as an immediate stop of steam delivered to a consumer at a certain point, which can occur if a paperboard machine suddenly stops, and has no need for steam in the drying process. Due to inertia within the system, the load is gradually lowered. Hence, gradually lowered steam demand was used in the simulation as well. After the model reached steady state again, the start-up of the load was initiated. The load connected to the 3 bar header was then gradually ramped up until the steam demand was reached.

The second operating case also consisted of a load trip and a load start-up of the load on the 3 bar header, and additionally included noise, which the first case did not have. Noise was added on all the loads in the model where the fluctuations were up to 10 kg/s on the lower pressure headers 3 bar and 8 bar, and the 12 bar and 17 bar headers fluctuated maximum 5 kg/s. The added noise values were defaults in the existing Dymola model and were introduced to the model to investigate how disturbances that exist in a non-ideal process affect the modified control system. Figure 4.1 and Figure 4.2 show the 3 and 12 bar header with noise presented in red and without noise seen in blue.

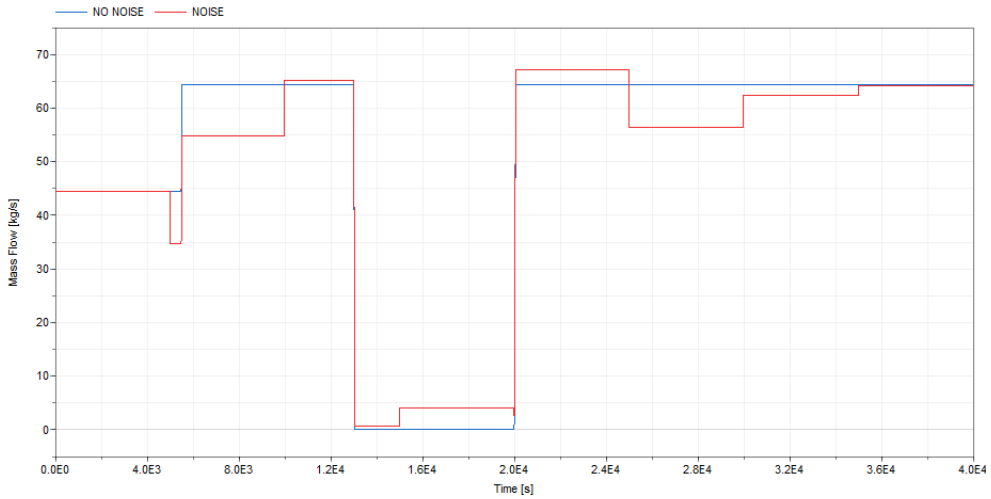

Figure 4.1: Load on the 3 bar header during load trip and load start-up.

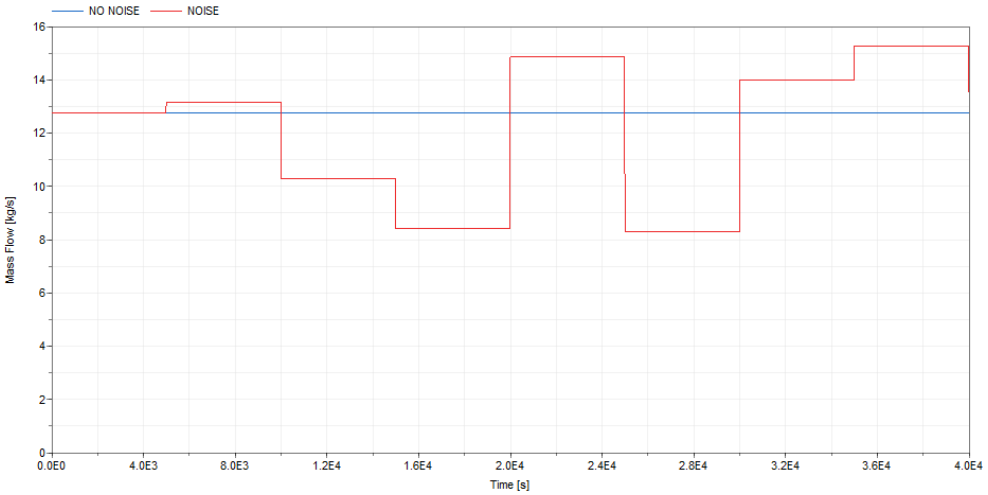

Figure 4.2: Load on the 12 bar header during load trip and load start-up.

Lastly, the third and final operating case dealt with a partial turbine trip where the 65 bar header closed its inflow valves to the turbine. This was done to illustrate how the control system performs when the turbine, which is a central component in the system, is out of service.

The efficiency of the steam system was determined by first collecting the following data from the simulations: the mass flow through the pressure relief valves, fuel input in terms of mass flow, and electricity generation. The data was then used to calculate the heat loss through the pressure relief valves Q_{loss} and the internal energy in the oil input to the boilers Q_{fuel}. Equation (2.3) was used to calculate Q_{fuel}, where LHV was gathered for the different fuels, i.e., oil, black liquor, and bark [20], [**Bajpai2018BiermannsPaper**] [21]. Equation (2.1) was used to obtain Q_{loss}. The Δh denotes the difference in enthalpy between the steam from the 3 bar header at 160°C and steam in the atmosphere at 1 bar and 10°C. Finally, the energy utilisation factor EUF was calculated according to Equation (2.2), where the utilised energy Q_u was defined as the difference between Q_{fuel}

and Q_{loss}. Since each operating case has different simulation times, the variables Q_{loss}, Q_{fuel}, and P_{el} were normalised per time unit in order to better evaluate the effect of each implementation and to easier compare among themselves.

To evaluate the control quality of the system, the integrated absolute error (IAE) for each pressure header was calculated according to

$$IAE = \int_{t_{i-1}}^{t_i} \mid e(t) \mid dt \tag{4.1}$$

IAE is the accumulated absolute error e between the process value and the set point in terms of pressure during simulation time t [22]. By comparing the IAE between the implementation and the reference model, any improvement was feasible to assess.

The change of IAE, i.e., ΔIAE, during different operating cases was evaluated with

$$\Delta IAE = \frac{IAE_{ref} - IAE_{imp}}{IAE_{ref}}, \tag{4.2}$$

where IAE_{ref} is the IAE for the reference case and IAE_{imp} for the new implementation.

Furthermore, the maximum pressure error on each header during the simulation time t was measured for the implementation and reference respectively for each studied case. The values were then used to calculate the change of the maximum error, i.e.,

$$\Delta \mid e(t) \mid_{MAX} = \frac{\mid e(t)_{ref} \mid_{MAX} - \mid e(t)_{imp} \mid_{MAX}}{\mid e(t)_{ref} \mid_{MAX}}. \tag{4.3}$$

5

Implementations

The following chapter explains in detail the model execution of three selected ideas based on the research questions presented in Section 1.2. Modifying the opening sequence of the reduction valves 65/3, changing the control hierarchy for the 65 bar controller, and changing the control hierarchy for the 12 and 3 bar controllers were the new strategies implemented in Dymola.

5.1 Opening Sequence of Reduction Valves 65/3

The first selected idea concerned the opening sequence of parallel reduction valves between two headers. In the original steam system, the valves open serially when several parallel reduction valves are installed. This implies that the second valve remains closed until the first valve is fully opened, as seen in Figure 5.1. Theoretically, a serial opening sequence leads to a linear correlation between the control signal and the mass flow for linear valves. However, when valves have non-linear characteristics, the mass flow is not linearly dependent on the control signal. The given valve characteristic, illustrated in Figure 5.1, had less response at the smallest and largest opening degrees, whereas the response was more linear around an opening degree of 50%.

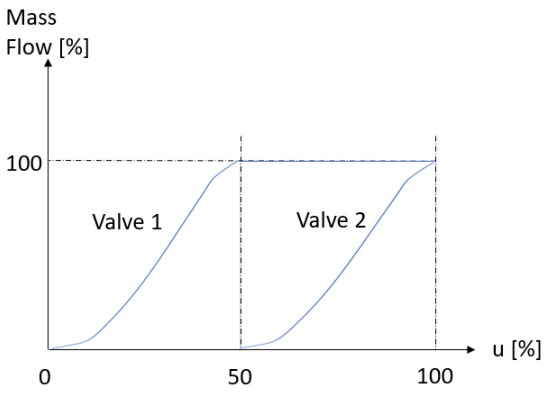

Figure 5.1: Illustration of serial opening sequence of two non-linear valves.

Based on data given on how a valve characteristic may look, an overlapping opening sequence of the reduction valves was developed in MATLAB to achieve a more linear

response of the control signal. By allowing the opening of the valves to overlap, a more linear response may be achieved when a steam header requires more steam or needs to dispose steam. In the long run, this can increase control quality in the steam net as deviation and duration are reduced. The non-linearity first appeared in the actuator in the steam system model while the control system assumed linear valves. However, the overlap opening was introduced in the control system to compensate for the non-linearity beforehand. In Figure 5.2a, it can be seen that a reduced range of the control signal was used when an overlap was present. As a consequence, a deadband appeared seen in grey between 80 and 100% in Figure 5.2a, which was removed by rescaling the control signal. This was done by reducing the size of the total valves, i.e., reducing the range of the control signal for the 3 and 65 bar controller. The overlap opening of two valves without a deadband is presented in Figure 5.2b.

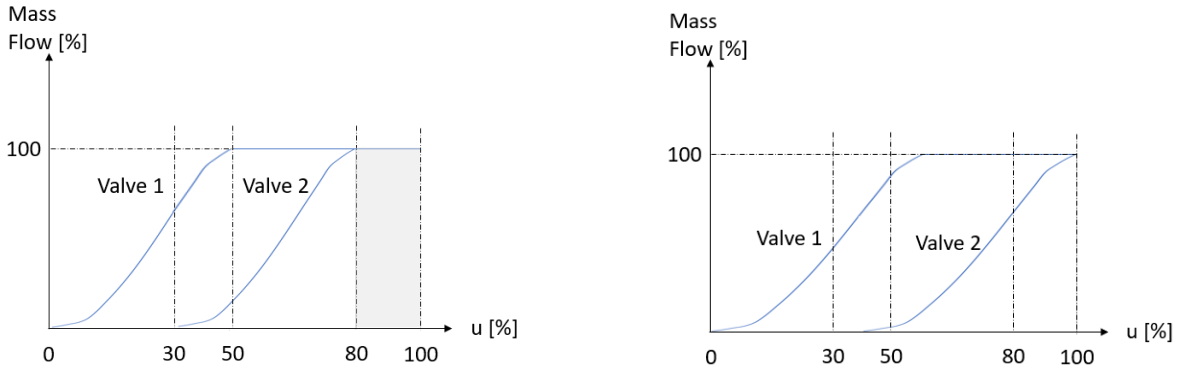

(a) Overlap opening of two valves without rescaled control signal.

(b) Overlap opening of two valves with rescaled control signal.

Figure 5.2: Overlap opening of two valves without and with rescaled control signal.

In Figure 5.3, the correlation between the control signal and the total mass flow of two reduction valves is plotted. The dotted black line shows linear valves opening in serial and darker blue curve non-linear valves with serial opening. As can be seen, the non-linear valves opening in serial leads to a non-linear response. To determine where the second non-linear valve was supposed to open to get the most linear correlation, the root mean square error ($RMSE$) of two non-linear valves was calculated in MATLAB. The root mean square error was calculated according to Equation (5.1), where n is the number of data points, y_i the total non-linear mass flow in point i and $\hat{y}_i$ the total linear mass flow in point i. This was done for all possible overlaps between fully parallel to fully serial valve opening. The overlap with the smallest $RMSE$ determined where valve 2 should start to open to minimise the error. Further, since the given valve characteristic had a decline of mass flow when valve 2 almost was fully open, it was decided to restrict the non-linear valve 2 to a maximum opening degree of 80%. The mass flow was then restricted to 95% of the total mass flow of the valve. In this way, the linear correlation increased compared to only overlapping the opening degree of the two valves. The light blue curve in Figure 5.3 shows the final overlap valves with a restricted flow in valve 2 of maximum 95%.

$$RMSE = \sqrt{\frac{\sum_{i=1}^{n}(y_i - \hat{y}_i)^2}{n}} \tag{5.1}$$

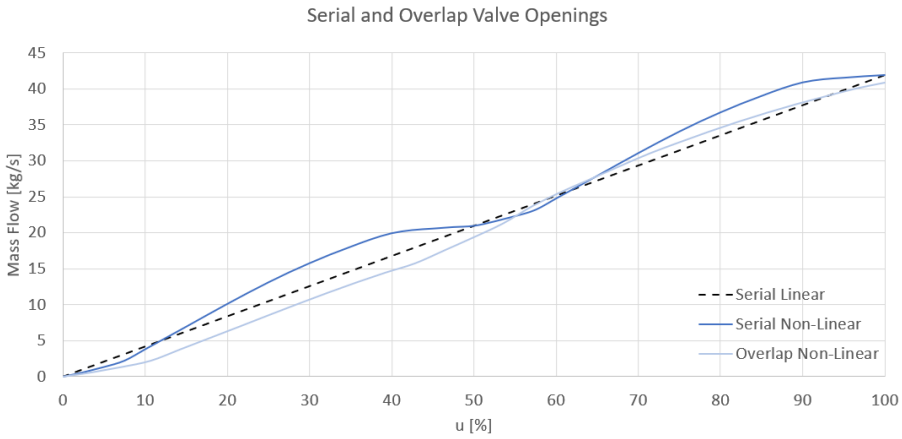

Figure 5.3: Graph over serial opening with linear and non-linear valves, and overlap opening of two non-linear valves.

5.2 Control Hierarchy for 65 Bar Header

In the second implementation, the control hierarchy in the 65 bar header was changed by adding a low limit split block for the 65/12 reduction valve between the turbine split block and the LL 65/8 reduction valve split block seen in Figure 5.4. When there is an excess of steam in the 65 bar header, the 12 bar header should receive the steam, which at an excess of steam forces the valve into the accumulator to open by its limit control. The desired outcome is that the accumulator will be filled faster leading to less fuel usage, and reduced use of the pressure relief valves on the 3 bar header.

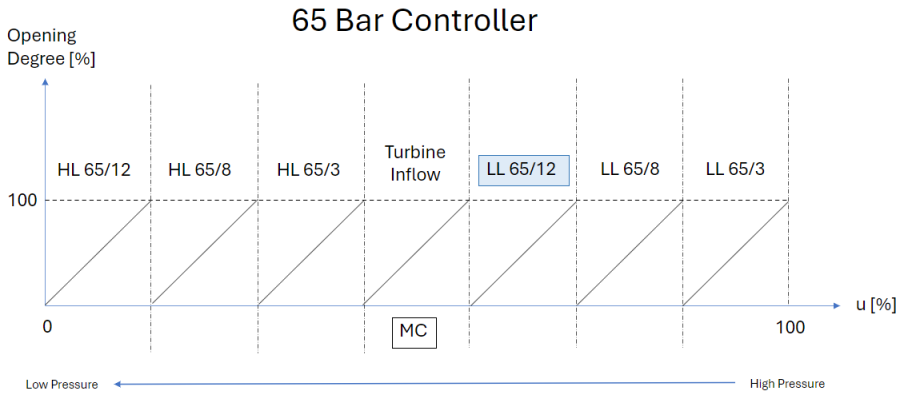

Figure 5.4: 65 bar controller with an added split block, coloured blue.

The new LL 65/12 split block added to the 65 bar controller is presented in Figure 5.5, where the maximum available mass flow in the valve between the 12 bar header and the accumulator is considered. The reason for this consideration is for the 12 bar header to be able to dispose steam during steam excess without affecting its pressure. As the 12 bar header experiences steam excess, its header can only dispose steam via the inlet accumulator valve since it does not have any reduction valves. The maximum available mass flow in the valve varies accordingly with the pressure drop over the valve, that is, the pressure drop between the 12 bar header and the accumulator.

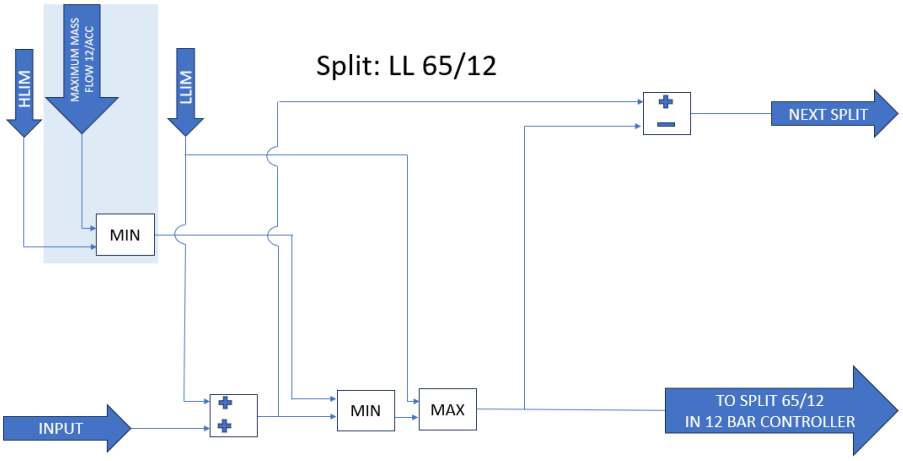

Figure 5.5: The low limit split block for reduction valves 65/12.

5.3 Control Hierarchy for 3 Bar & 12 Bar Header

Implementation 3 used different controllers to control the extraction valves between the turbine and the 12 bar header, and the accumulator inflow valve. Originally, the turbine extraction valves and the accumulator inflow valve were controlled from the 12 bar controller and 3 bar controller, respectively. The new implementation switched the control of these valves between the two headers. This means that the 12 bar controller controls the accumulator inflow, and the 3 bar controller controls the turbine extraction valves to the 12 bar header. Figure 5.6a illustrates the original 3 bar controller and Figure 5.6b shows the modified 3 bar controller with a new split block marked in blue.

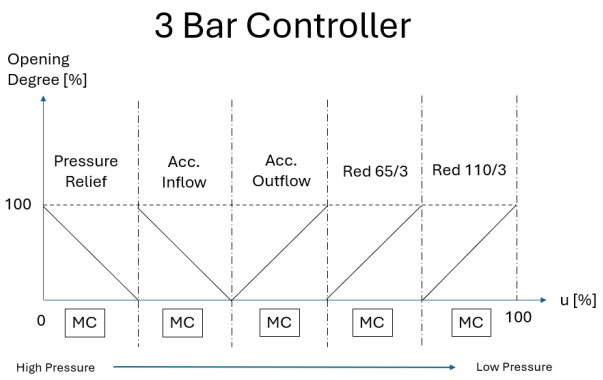

(a) Original 3 bar controller.

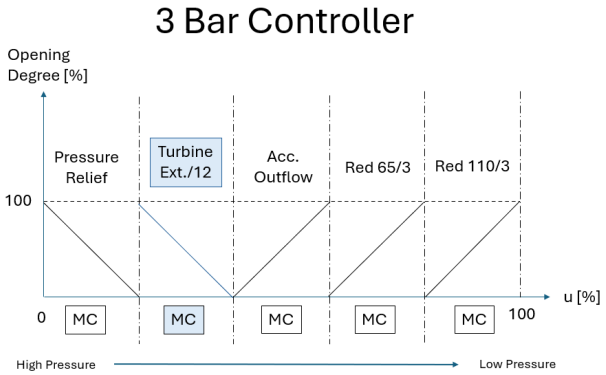

(b) Modified 3 bar controller.

Figure 5.6: Illustration of the 3 bar controller in the reference and modified case.

Figure 5.7a demonstrates the original 12 bar controller and in Figure 5.7b the modified control sequence for the 12 bar controller with two new split blocks added is seen. The first new block controls the accumulator inflow valve and the second controls the high limit for the extraction valves from the turbine to the 12 bar header. The high limit is a limit control for the 12 bar turbine extraction split block placed in the 3 bar controller. By adding a high limit block, the 12 bar header may prevent too high pressure caused by a surplus of steam if no more steam can enter the accumulator.

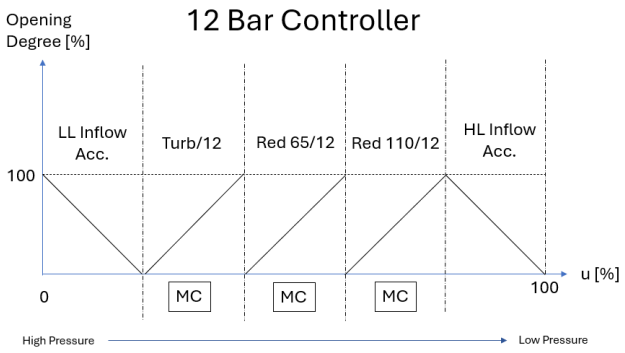

(a) Original 12 bar controller.

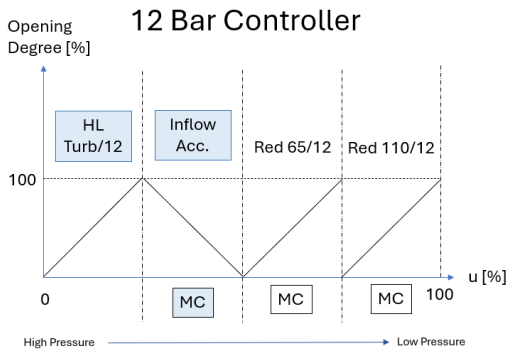

(b) Modified 12 bar controller.

Figure 5.7: Illustration of the 12 bar controller in the reference and modified case.

6

Results

During the simulation phase, the selected operating cases were considered individually for each of the three implementations. Since reduction valves are not used during load trips, this operating case was excluded for the first implementation. No result from the load trip was gathered during the second simulation either. This was because it was seen during the load trip on the 3 bar header that the production headers experienced a lack of steam, which is not desirable if the second implementation only can be tested when there is an excess of steam. Moreover, since the third implementation was connected to the turbine extraction valves, a turbine trip was not relevant for evaluating the implementation. Table 6.1 shows the operating cases that were tested in the implementations.

The key variables that were selected have different meanings whether they are positive or negative in the Tables 6.2, 6.4, and 6.6. The values are calculated based on a comparison between the reference and implementation model. High values of EUF and P_{el} are desirable since it means that the system is more energy efficient and has a higher electricity production. Therefore, an improvement in these variables should be denoted with positive values, showing an increase. The system losses Q_{loss} and oil fuel input Q_{fuel}, on the other hand, are aiming for negative values, since it is desirable to reduce steam losses and oil usage. Since the different operating cases were simulated during varied time lengths, these variables are divided by the simulation time to yield a result in average energy per unit time. Comparisons regarding IAE and maximum pressure error $|e(t)|_{MAX}$ are seen in Tables 6.3, 6.5, and 6.7. Positive values indicate that there is an improvement in the

Table 6.1: Visualisation of which operating cases that were tested in the implementations.

Implementation	Operating Cases		
	Load Trip	Load Start-up	Partial Turbine Trip
Opening Sequence of Reduction Valves 65/3		X	X
Control Hierarchy for 65 Bar Header			X
Control Hierarchy for 3 Bar and 12 Bar Header	X	X	

implementation compared to the reference and negative values a deterioration. All tables use colours to indicate if the implementation performed better or not. Green-coloured values indicate improvement, red-coloured values deterioration, and white no significant change.

6.1 Opening Sequence of Reduction Valves 65/3

Table 6.2 shows how the key variables were affected by the implementation in comparison to the reference. It is seen that the load start-up had different results between the models. The EUF, electricity generation, and oil fuel input were less in the implementation. Significant differences were found in the reduced use of oil by approximately 60 kWh/h and a reduced produced power of 46 kWh/h. The load start-up was simulated with a noise of 1.25 kg/s on the 3 bar header and 8 bar header, and 2.5 kg/s on the 12 and 17 bar headers. The noise that was simulated was lower compared to the noise presented in the method. The reason for this is that the implementation model could not handle large noise fluctuations due to software failure. Therefore, the noise was reduced until the simulation was able to be fully executed. Moreover, during the partial turbine trip, the variables were not significantly affected except for Q_{loss} which appeared to be lower in the implementation, and thus improved.

Table 6.2: Comparison of the key variables between the reference and implementation model.

Variables	Operating Case	Improvement
EUF [%]	Load Start-up	-0.009
	Partial Turbine Trip	0.004
Q_{fuel} [kWh/h]	Load Start-up	-59.49
	Partial Turbine Trip	-2.02
Q_{loss} [kWh/h]	Load Start-up	1.44
	Partial Turbine Trip	-8.37
P_{el} [kWh/h]	Load Start-up	-46.00
	Partial Turbine Trip	2.17

The pressure stability is seen in Table 6.3. During load start-up, IAE improved on all headers, and there was a significant improvement on the 65 bar header, where fluctuations were reduced by 22%. From the maximum pressure error perspective, the implementation showed a general improvement. The partial turbine trip did not have the same improvement, showing worse pressure stability on the 3, 12, and 65 bar header. However, the $\mid e(t) \mid_{MAX}$ was greatly improved by almost 16% on the 65 bar header.

Table 6.3: Comparison of the pressure stability between the implementation and reference during the partial turbine trip.

Variables	Operating Case	Pressure Header				
		3 bar	8 bar	12 bar	65 bar	110 bar
ΔIAE [%]	Load Start-up	6.0	7.1	3.5	22.2	2.7
	Partial Turbine Trip	-44.5	0.8	-8.1	-4.3	0.0
$\Delta \mid e(t) \mid_{MAX}$ [%]	Load Start-up	-0.3	2.6	0.6	18.3	11.9
	Partial Turbine Trip	0.6	1.0	0.0	15.6	0.0

6.1.1 Load Start-up

In Figure 6.1, the pressure levels for the 65 and 3 bar headers are shown for the simulations with noise. It can be seen that the pressure generally fluctuates less on the 65 bar header in the implementation, whereas no large visual difference was seen in the 3 bar header.

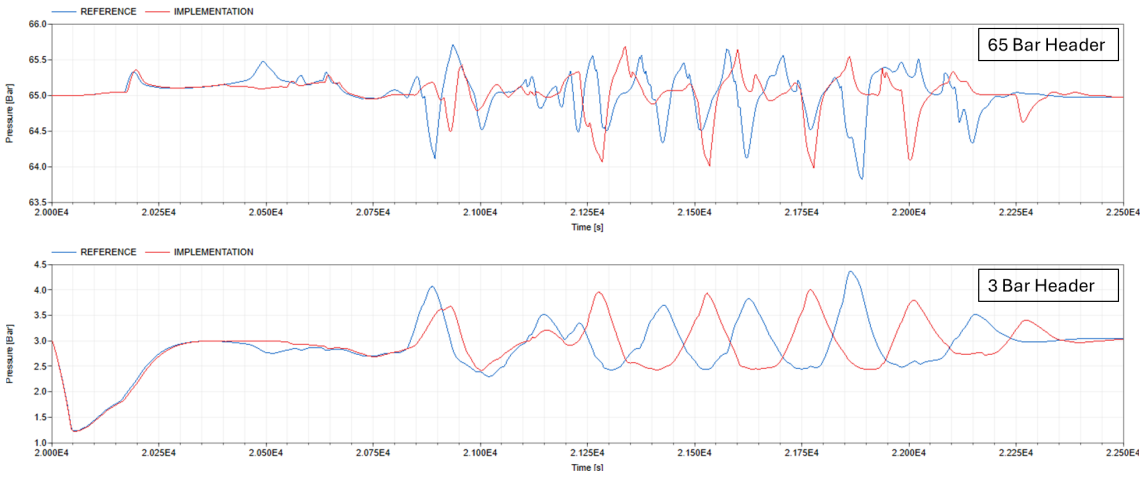

Figure 6.1: Pressure levels on the 65 bar header and 3 bar header.

During load start-up with noise, the reduction valves 65/3 were used as seen in Figure 6.2 and Figure 6.3. Both the opening degree of valve 1 and the total mass flow in 65/3 fluctuated more in the implementation than in the reference. However, Figure 6.3 shows that a more linear opening of the valves during load start-up was achieved in the implementation.

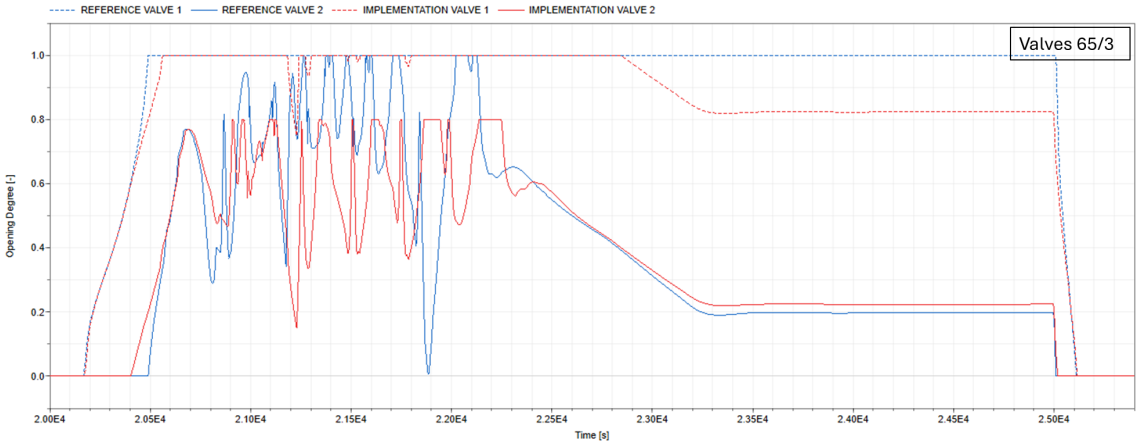

Figure 6.2: Opening degree of 65/3 reduction valves with noise.

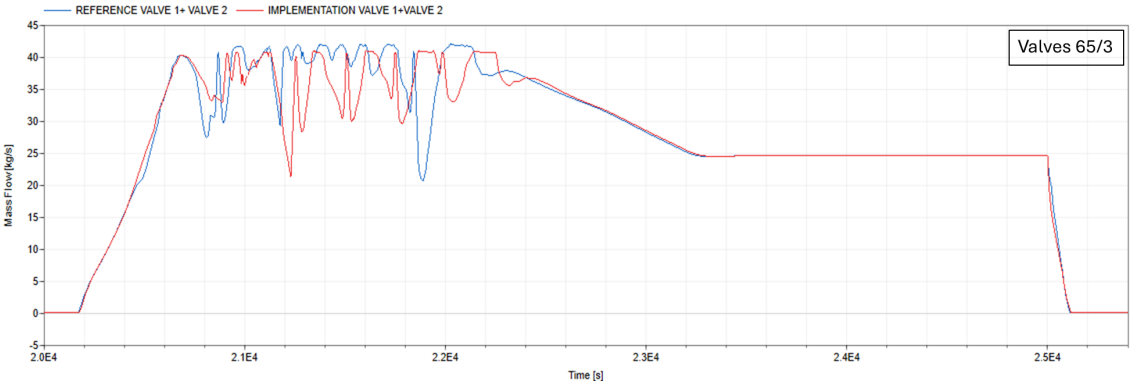

Figure 6.3: Total mass flow in reduction valves 65/3 with noise.

6.1.2 Partial Turbine Trip

The pressure headers connected to the modified valves are seen in Figure 6.4. It is seen that the implementation model had a lower $\mid e(t) \mid_{MAX}$ on the 65 bar header and larger fluctuations on the 3 bar header.

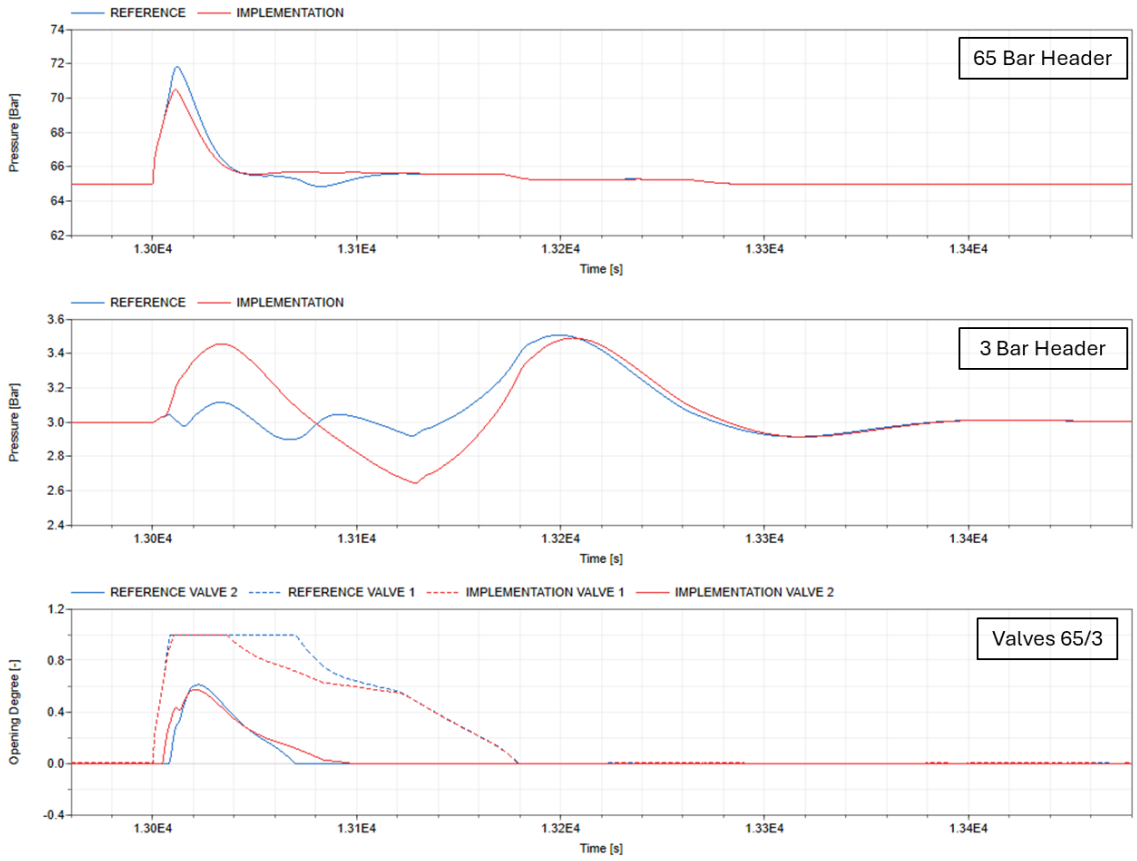

Figure 6.4: Pressure headers for 65 and 3 bar, and opening degrees of valves 65/3 for the reference and implementation.

Figure 6.5 shows the result of the total mass flow through the two valves between the 65 bar and 3 bar header in the reference and implementation. As expected, the implementation had a faster response in terms of mass flow.

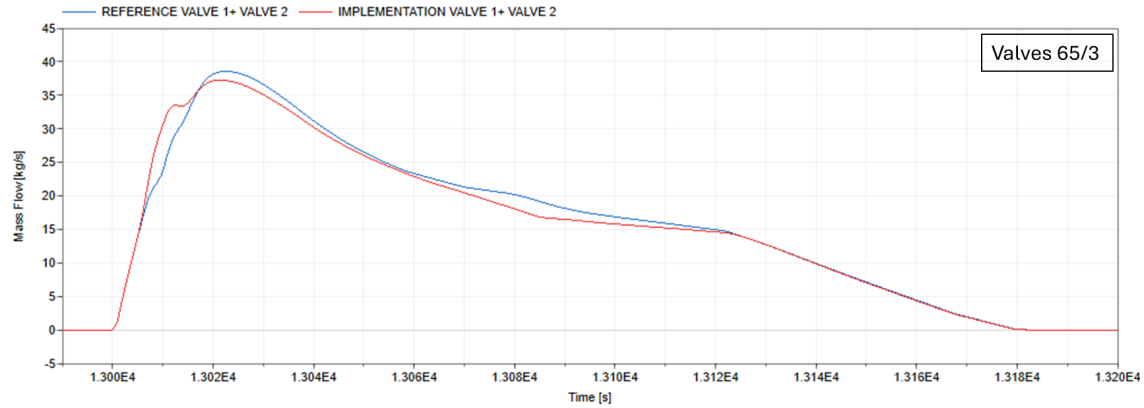

Figure 6.5: Total mass flow through the two reduction valves 65/3.

6.2 Control Hierarchy for 65 Bar Header

Table 6.4 shows how the key variables in the implementation compare to the reference model. It is seen that electricity generation was largely increased by 1550 kWh/h as well as the oil fuel input by almost 1700 kWh/h in the implementation. The EUF was improved by 0.54% and less steam losses Q_{loss} was observed.

Table 6.4: Comparison of the key variables between the reference and implementation model.

Variables	Operating Case	Improvement
EUF [%]	Partial Turbine Trip	0.545
Q_{fuel} [kWh/h]		1687.42
Q_{loss} [kWh/h]		-37.08
P_{el} [kWh/h]		1550.41

From Table 6.5 it is seen that all pressure headers were improved from both the IAE and the maximum pressure error perspective. The largest improvement is seen in the 8 bar header where ΔIAE increased by 38% and the maximum pressure error by 20%. The 110 bar header remained almost unchanged but with a slight improvement of its maximum error that was 3% lower compared to the reference.

Table 6.5: Comparison of the largest pressure error and IAE between the implementation and reference during the partial turbine trip.

Variables	Operating Case	Pressure Header				
		3 bar	8 bar	12 bar	65 bar	110 bar
ΔIAE [%]	Partial Turbine Trip	22.0	38.3	28.3	9.2	0.5
$\Delta \mid e(t) \mid_{MAX}$ [%]		23.4	20.4	17.2	8.4	3.0

In Figure 6.6, the pressure levels of the 65 bar header and the 12 bar header are presented as well as the mass flow through reduction valve 65/12 during a partial turbine trip without noise. The implementation appeared to reach a slightly lower maximum pressure peak at the 65 bar header than the reference. Regarding the 12 bar header, the implementation fluctuated more, but with lower maximum error. The 65/12 reduction valves were used to a larger extent in the implementation through the partial turbine trip.

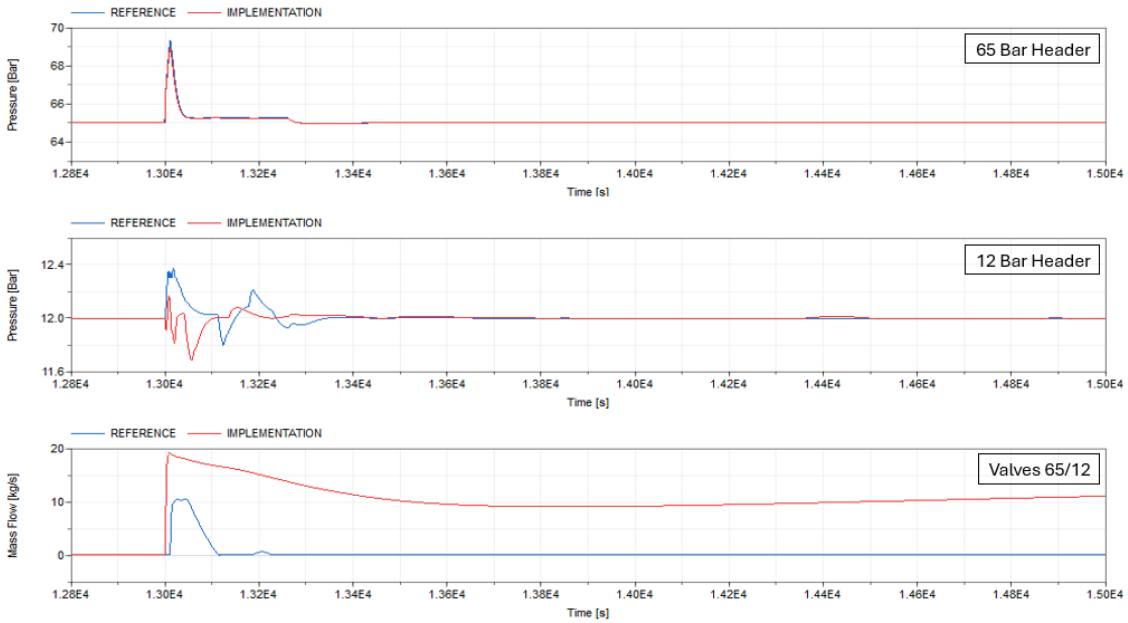

Figure 6.6: Pressure on 65 bar header and 12 bar header, and mass flow through reduction valves 65/12.

The accumulator pressure, visible in Figure 6.7, was lower in the implementation, although the inlet valve to the accumulator was used more after 15 000 s in the implementation. However, at the same time, the outlet valve was used, leading to a decreased accumulator pressure.

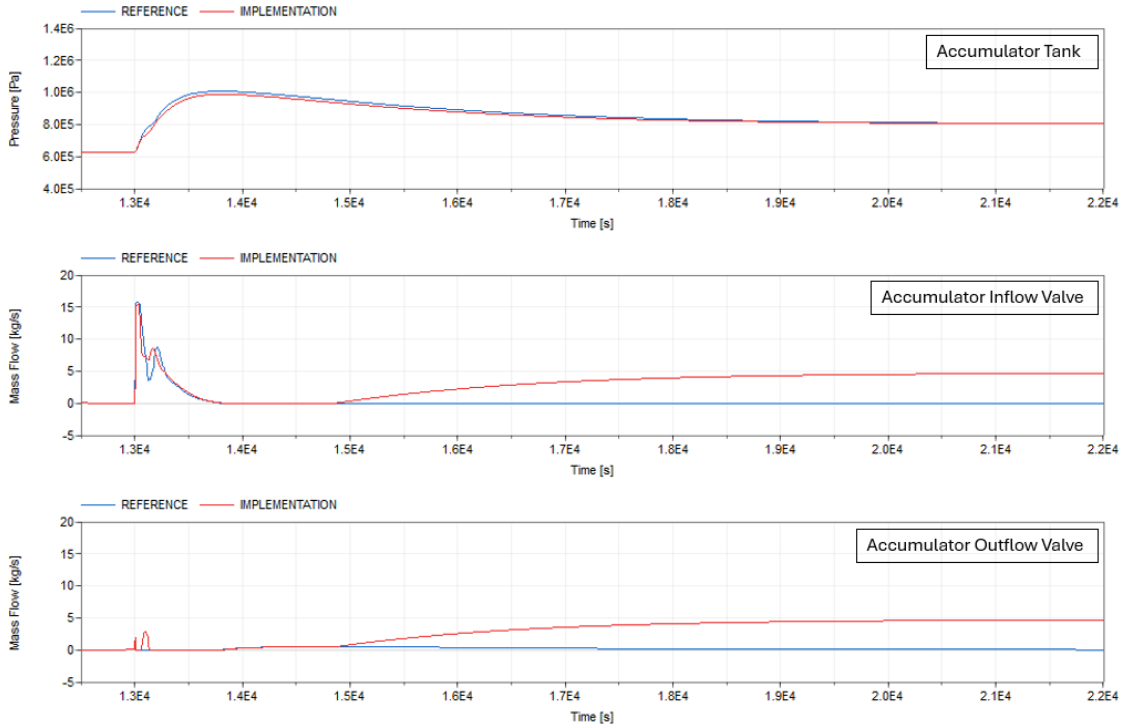

Figure 6.7: Accumulator pressure, and mass flow through the accumulator inlet and outlet valves.

It can be seen in Figure 6.8 that the 12 bar turbine extraction reduced significantly in the implementation. Meanwhile, the mass flow through the 8 bar turbine extraction valves was larger in the implementation. The remaining mass flow to the 3 bar header was firstly a bit higher in the implementation and then remained at a constant mass flow in both models.

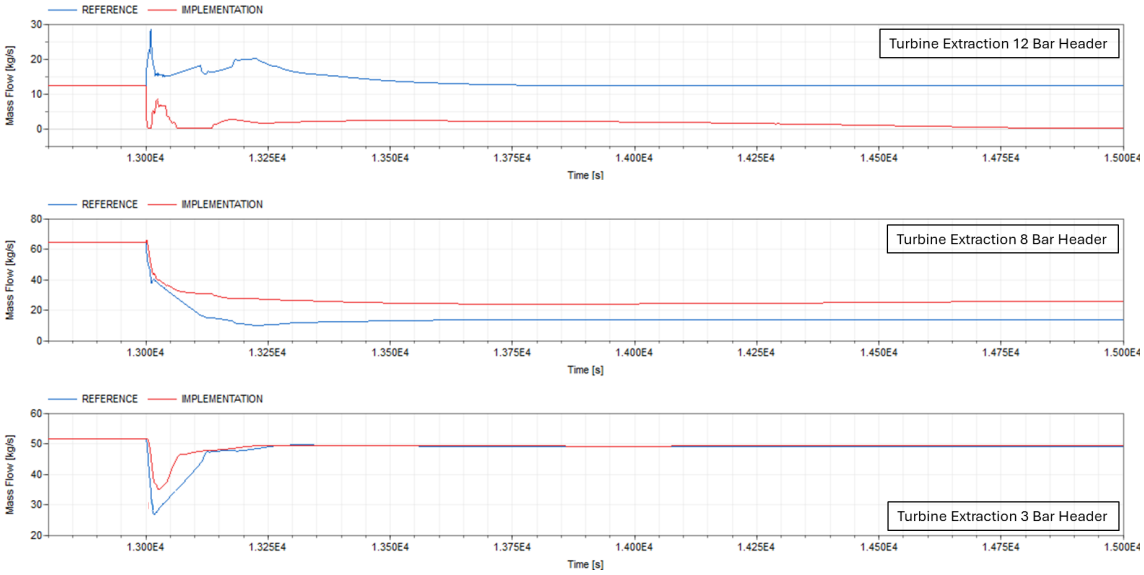

Figure 6.8: Turbine extraction at 12 bar, 8 bar and 3 bar.

Furthermore, the pressure level on the 8 bar header and 3 bar header fluctuated less in the implementation, according to Figure 6.9.

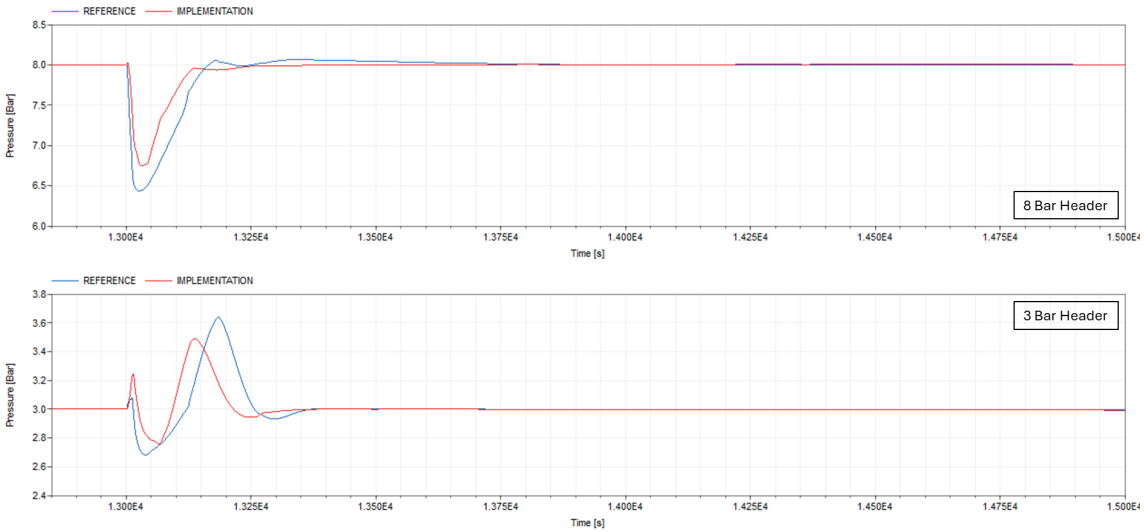

Figure 6.9: Pressure on 8 bar header and 3 bar header.

6.3 Control Hierarchy for 3 Bar & 12 Bar Header

The key variables for implementation 3 and its reference are shown in Table 6.6. It is seen that oil usage, steam losses and electricity generation are reduced in the implementation model during both operating cases. Meanwhile, EUF was better during the load trip and slightly deteriorated during load start-up. The simulations had noise fluctuations of 5 kg/s on the 3 bar and 8 bar header, and 10 kg/s on the 12 bar and 17 bar header.

Table 6.6: Comparison of key variables between the implementation and reference during load trip and load start-up with noise present.

Variables	Operating Case	Improvement
EUF [%]	Load Trip	0.183
	Load Start-up	-0.069
Q_{fuel} [kWh/h]	Load Trip	-859.01
	Load Start-up	-429.46
Q_{loss} [kWh/h]	Load Trip	-780.74
	Load Start-up	-11.40
P_{el} [kWh/h]	Load Trip	-177.43
	Load Start-up	-324.92

A comparison of the pressure stability between the reference model and the implementation model is seen in Table 6.7. The majority of the pressure headers fluctuate more over time in the implementation, as can be seen in the negative values marked in red. The largest deterioration during the load trip is seen on the 12 bar header, which was 58% worse or more. However, the 8 bar header had a great improvement during load start-up both in the values of IAE and the maximum amplitude error.

Table 6.7: Comparison of pressure fluctuations between the implementation and reference during load trip and load start-up with noise present.

Variables	Operating Case	Pressure Header				
		3 bar	8 bar	12 bar	65 bar	110 bar
ΔIAE [%]	Load Trip	-12.4	-3.0	-58.3	-0.6	0.8
	Load Start-up	-37.7	70.8	-74.1	-1.1	-23.8
$\Delta \mid e(t) \mid_{MAX}$ [%]	Load Trip	-8.8	-23.0	-59.7	-38.8	0.1
	Load Start-up	8.1	67.9	-57.5	-1.1	-14.1

6.3.1 Load Trip

In Figure 6.12, visual results of the values in Table 6.7 are seen with larger pressure fluctuations in the 12, 8, and 3 bar headers for the implementation. The 3 bar header increased its pressure slower than the reference and also had a larger pressure error.

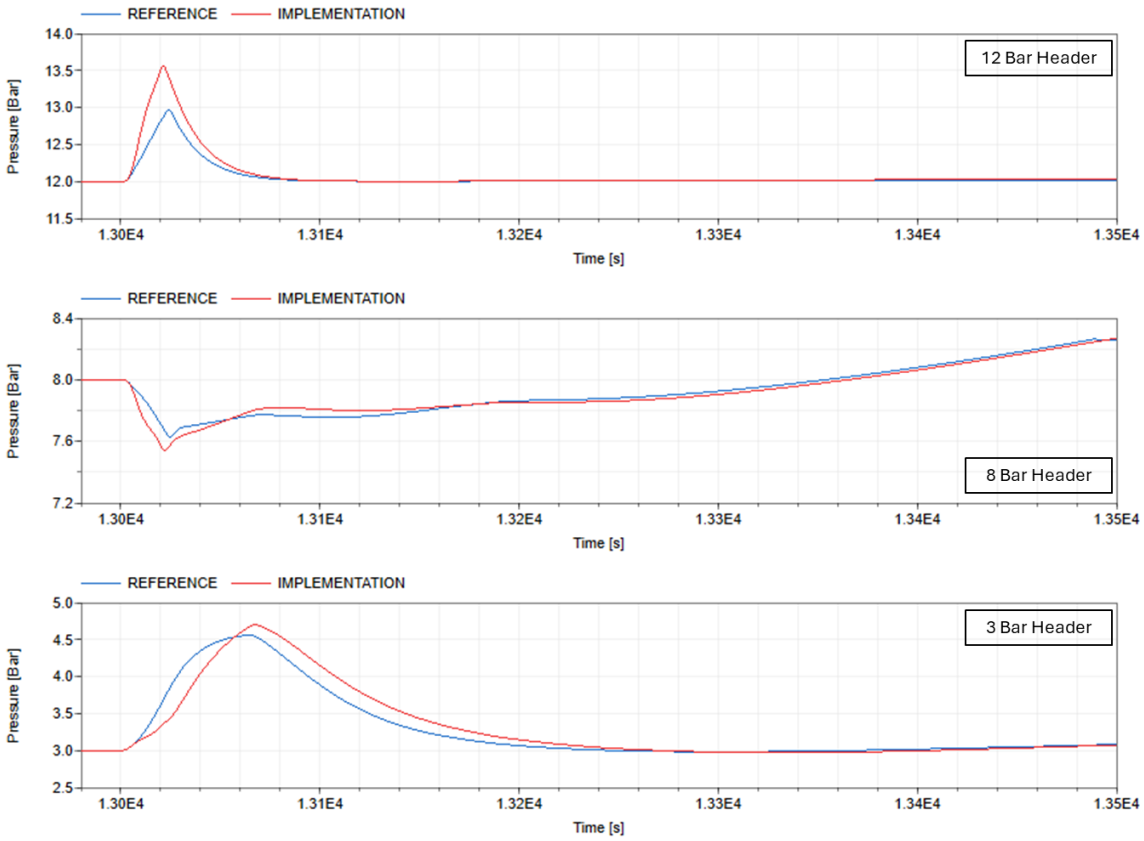

Figure 6.10: Pressure at the 12, 8, and 3 bar header with noise present.

The valve into the accumulator opened earlier, and the steam inflow increased faster as a consequence as seen in Figure 6.11. Before the load trip, the implementation model had a lower accumulator pressure and when the load trip occurred, the pressure had a faster growth compared to the reference.

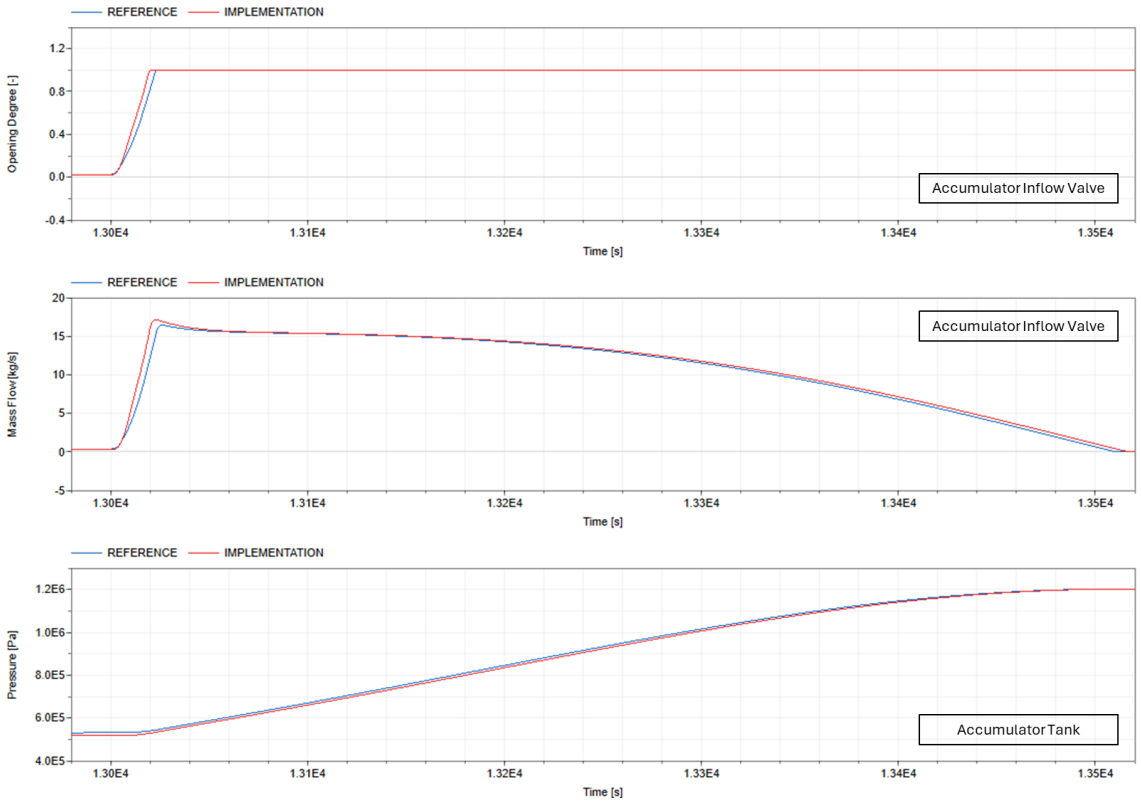

Figure 6.11: Accumulator inflow and pressure with noise present.

During the load trip (see Figure 6.12), the turbine extraction had a faster response in the implementation model. The 12 bar header increased its steam extraction faster and the 8 bar header decreased its steam extraction faster as a result. The turbine extraction to the 3 bar header decreased slightly faster during the load trip, and after 13 020 s it increased during a short time span, which is not seen in the reference model.

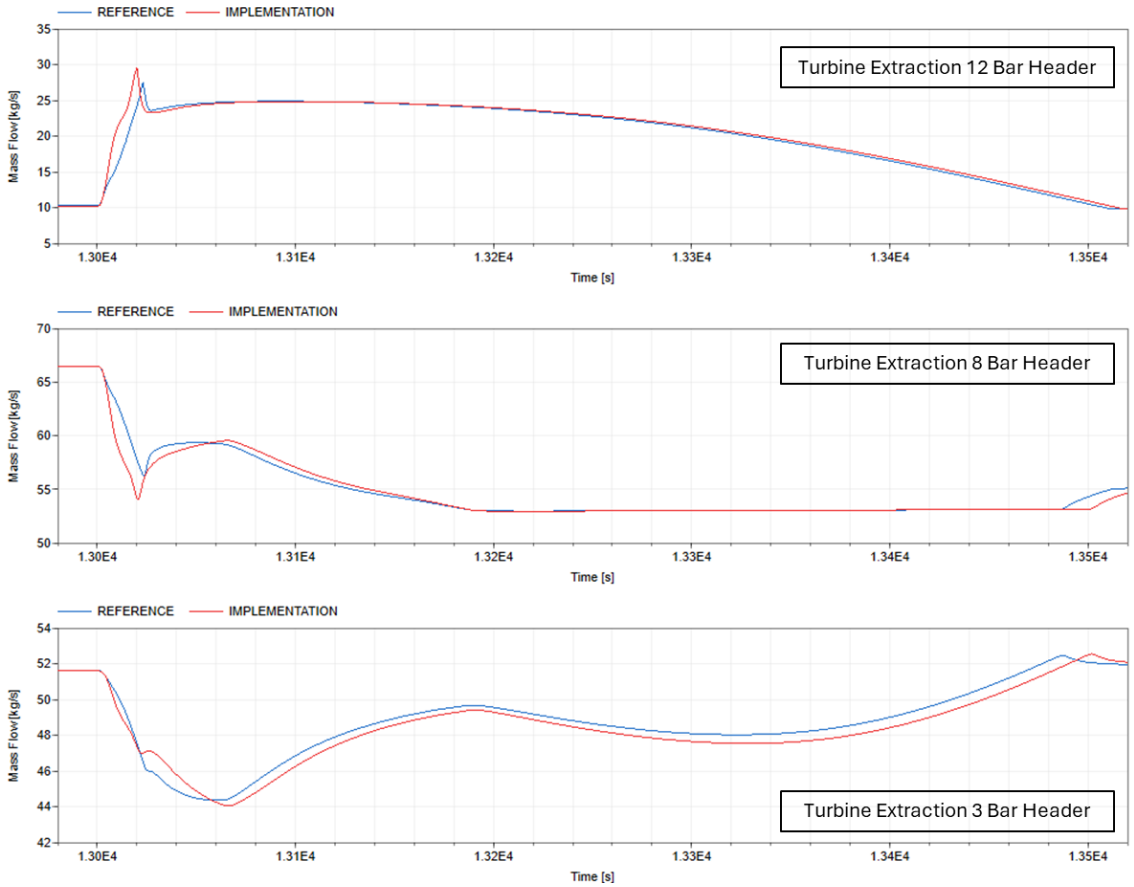

Figure 6.12: Turbine extraction to the 12, 8, and 3 bar header with noise present.

6.3.2 Load Start-up

As shown in Figure 6.13, the pressure in the 12 bar header fluctuated more during load start-up in the implementation. In contrast, the implementation had a more stable 8 bar header pressure. No significant difference in the 3 bar header pressure is seen between the implementation and the reference.

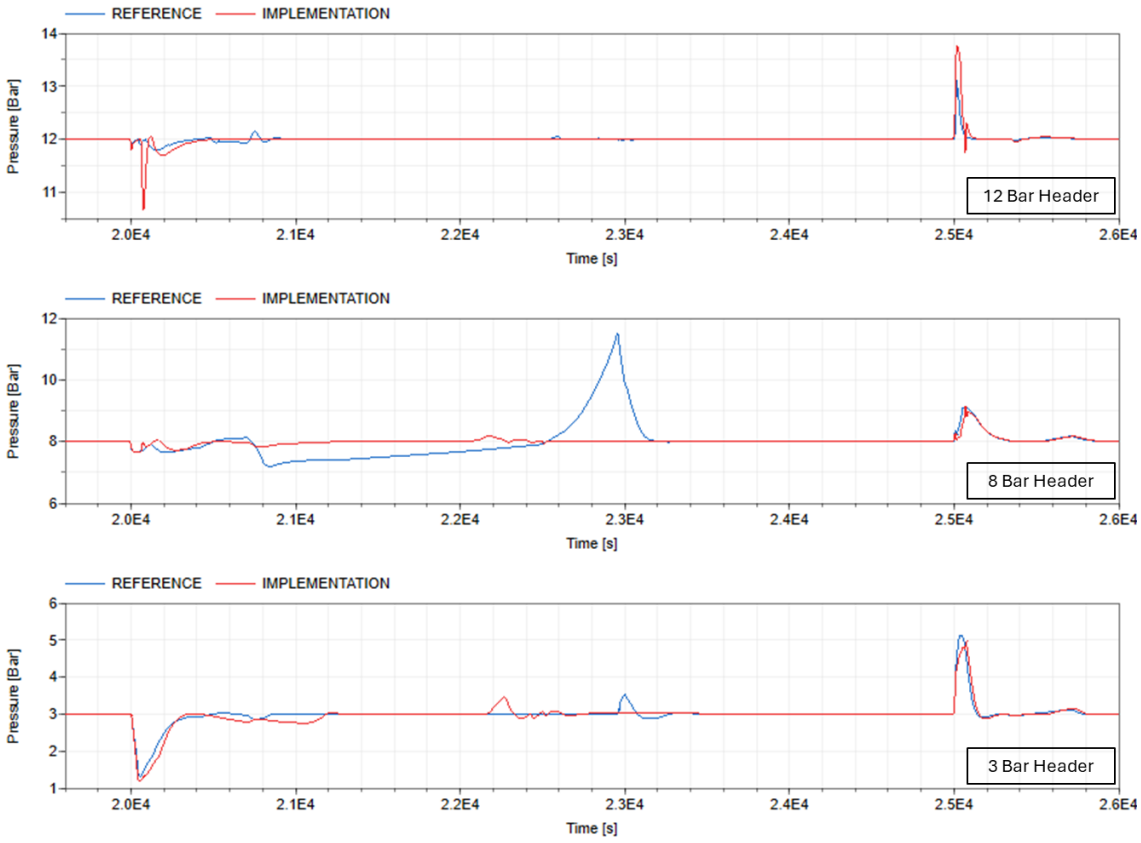

Figure 6.13: Pressure on the consumer headers for load start-up with noise.

In Figure 6.14, plots of the accumulator inflow valve in terms of opening degree and mass flow, and the accumulator pressure are presented. The inflow valve responds similarly in both models. The pressure of the accumulator tank changed slightly slower in the implementation.

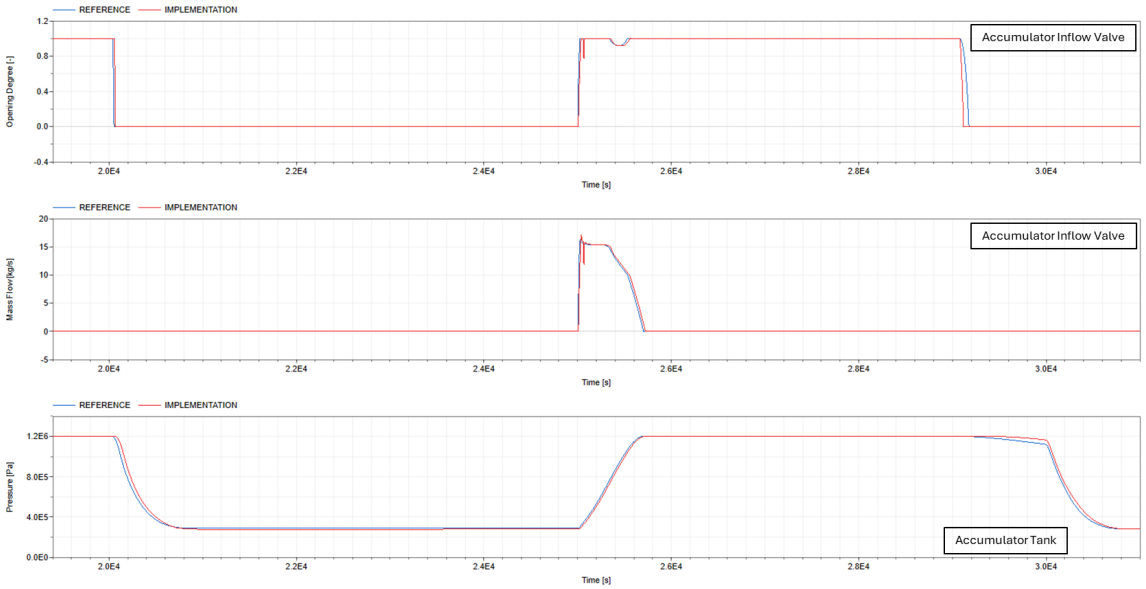

Figure 6.14: Opening degree and mass flow of the accumulator inlet valve, and pressure in the accumulator tank.

The turbine extractions to the consumer nets during load start-up with noise are shown in Figure 6.15. It can be seen that the extraction valves to the 12 bar header were closed in the implementation while they continued to be open in the reference model. The 8 bar turbine extraction valves had first a faster mass flow decrease in the reference seen after just over 22 400 s. Later at 22 200 s, a fluctuation occurred in the implementation. The 3 bar turbine extraction valves, which the 8 bar header controls, were closed in both models. However, the same valves opened earlier in the implementation.

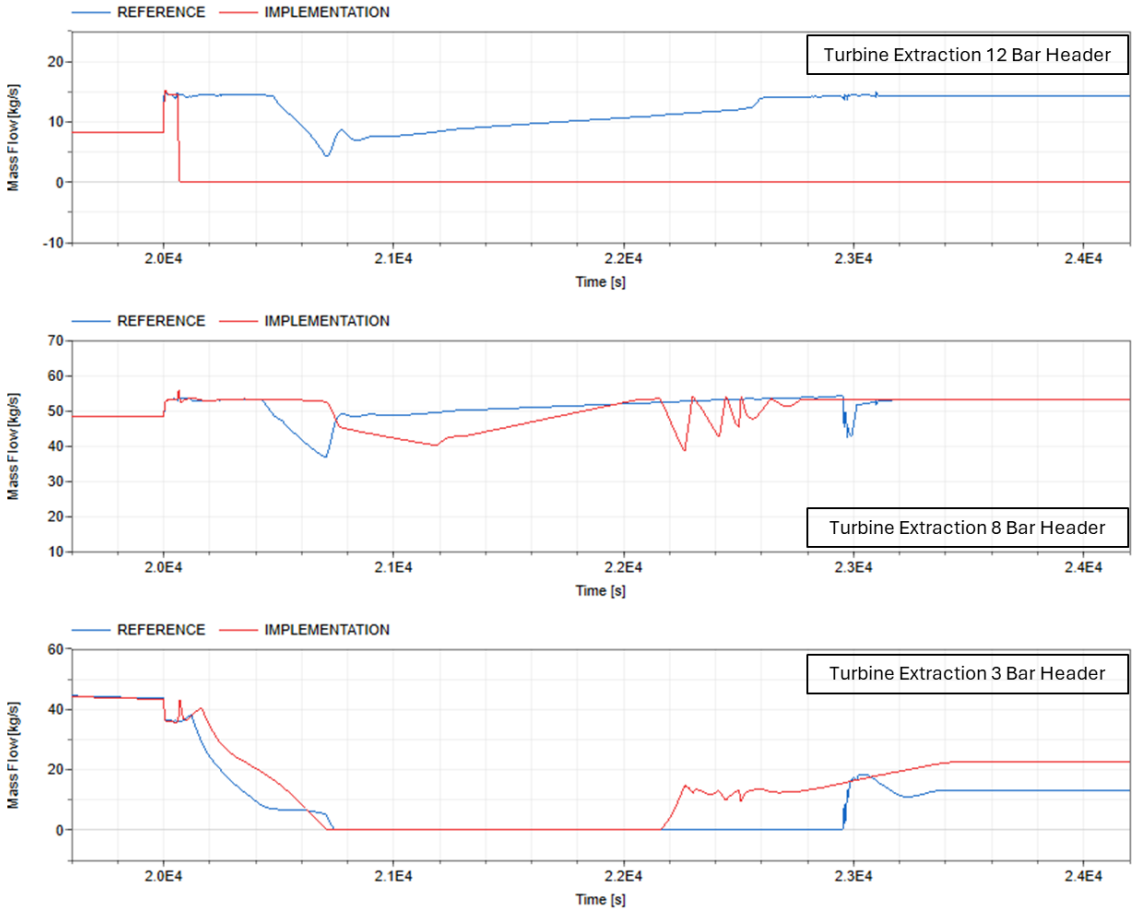

Figure 6.15: Turbine extraction to the consumer nets during load start-up with noise.

Furthermore, the turbine inflow valves had generally a smaller mass flow in the implementation than in the reference, as portrayed in Figure 6.16.

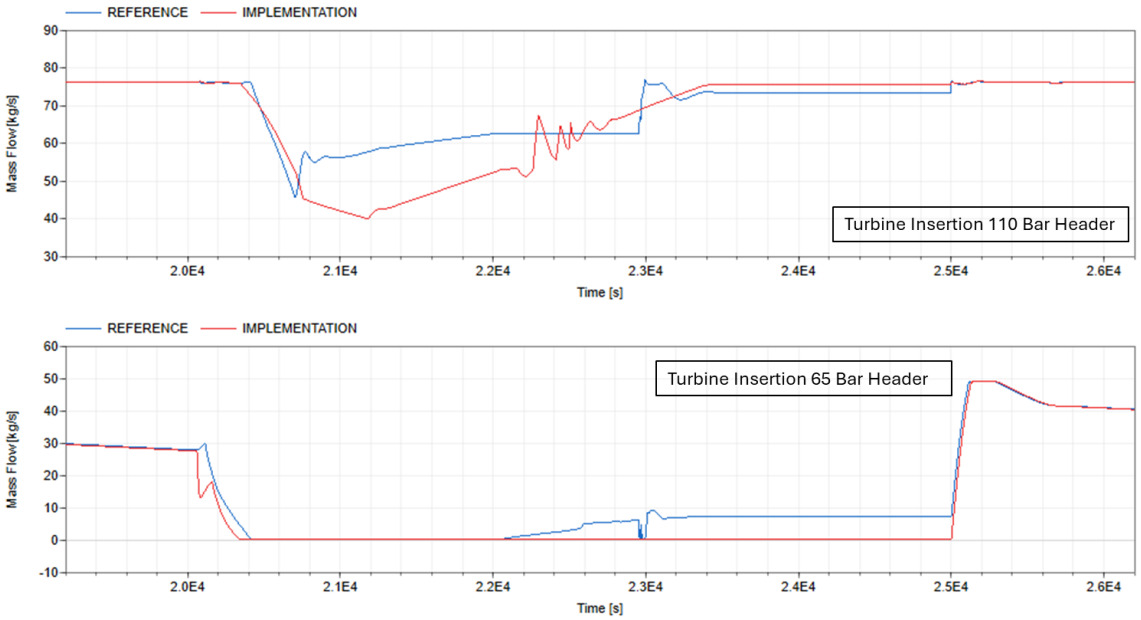

Figure 6.16: Turbine insertion from the 110 bar header and 65 bar header.

The usage of the reduction valves 110/3, 65/12 and 65/3 varied between the reference and implementation, as illustrated in Figure 6.17. Mainly, reduction valves 65/12 were used more in the implementation, and in contrast, the valves 65/3 were used slightly less. Reduction valves 110/3 opened slower and fluctuated more in the implementation.

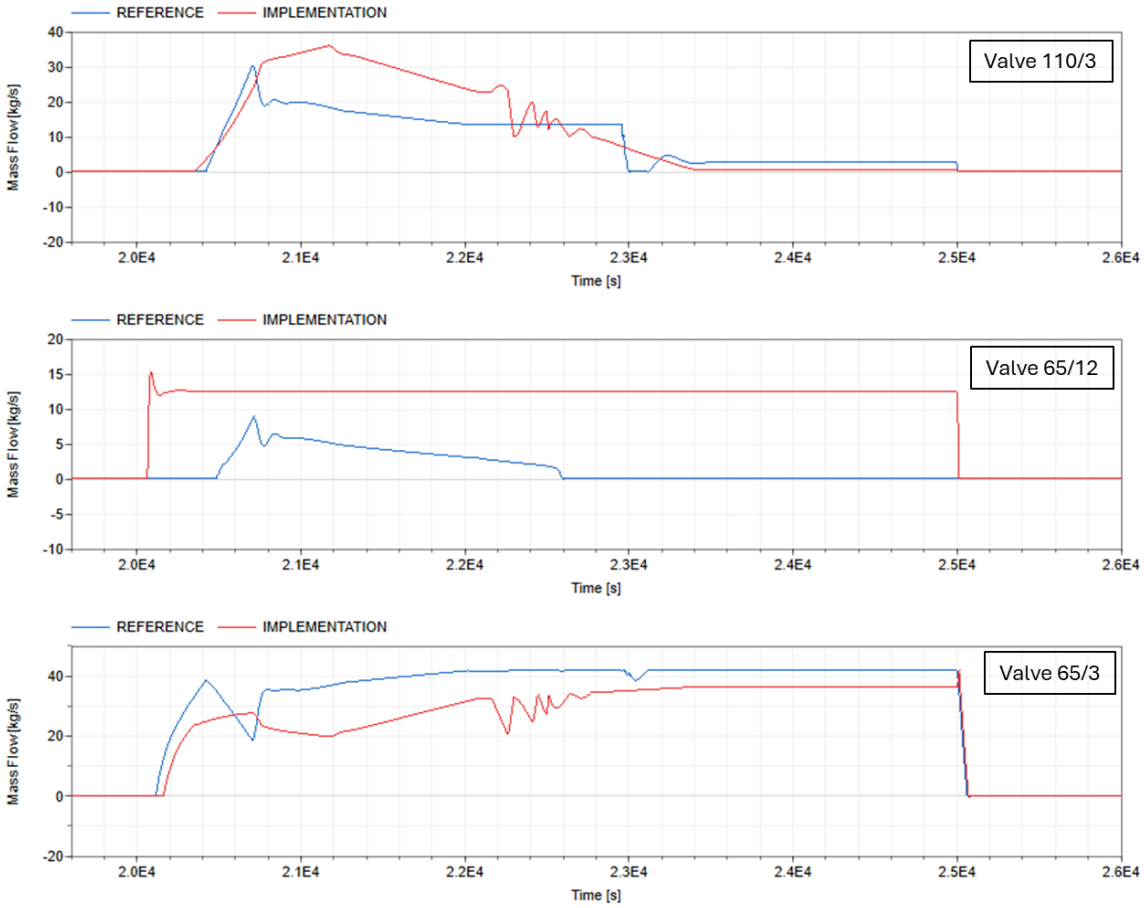

Figure 6.17: Mass flow in reduction valves 110/3, 65/12, and 65/3.

7

Discussion

In this section, the results of the thesis are analysed and evaluated. The three implementations are discussed based on the key variables and from a stability perspective. From the simulations, it was observed that the noise added during load trips and load start-ups had a long duration and amplitude, which may not represent disturbances that are realistic to occur in the existing system. However, it may still give a good indication of how well the system performs during stress. Simulating stress tests can be beneficial for comprehending the limits within the system. In the first implementation, limits of the system were achieved at a lower noise than in the third implementation, hence the varied noise magnitude between the simulations.

7.1 Opening Sequence of Reduction Valves 65/3

From the results of the first implementation, it is seen that the pressure stability in general has been improved. As previously stated, the overlap added in the control system is compensating for the non-linear characteristics in the reduction valves beforehand, which yields a more linear response between the mass flow through the valves and control signal. However, as a consequence of restricting valve 2 to being open no more than 80%, the total valve sizes in the 3 and 65 bar controller were changed. This change requires re-tuning of the controllers which has not been done. The current controllers are set to distribute a certain mass flow between the split blocks, and if the mass flow decreases, the controllers would be more sensitive to changes as it has less available mass flow to play with.

7.1.1 Load Start-up

The EUF was not significantly changed during load start-up, as seen in Table 6.2. However, fuel usage and electricity generation were reduced. Since the aim was to minimise the oil usage while improving or maintaining the stability of the system, the results were aligned with the purpose of the implementation. The electricity generation is secondary to providing the loads with steam, and therefore the implementation can be seen as beneficial since it prioritises the steam supply over generating electricity, although the EUF remained unchanged. Thus, undesired electricity generation from fossil fuels is minimised.

As seen in Table 6.3, the pressure stability was improved in the implementation during load start-up. The largest improvement is seen in the 65 bar header where ΔIAE was improved by 22%. This could be due to a faster and more linear response in mass flow when the valves had an overlapping opening sequence. The IAE of the 3 bar header was also improved, although it was a smaller improvement of 6%. Presumably, the marginal progression is due to a simplification where the added mass flow in the reduction valves is not considered. The production nets extract the requested steam that the consumer nets require without considering the water injected in the reduction valves to reduce the pressure and temperature of the steam. As a consequence, the consumer net receives larger amount of steam than requested, leading to an increased instability which reduces the benefits of the implementation.

In the results, the implementation tended to give a more linear mass flow when the valves opened around 20 000 s - 20 700 s, according to Figure 6.3. This is due to valve 2 which opened at a lower control signal in the implementation. As desired, when the mass flow rate in valve 1 declined, valve 2 opened to compensate for the non-linearity, resulting in a more linear total mass flow through the 65/3 reduction valves.

A drawback with an overlapping opening sequence of the reduction valves is that both valve 1 and valve 2 are used more often for regulating the mass flow. Figure 6.2 shows accordingly that the opening degree of valve 1 fluctuated more in the implementation compared to the reference. This could lead to wear due to rapid opening and closing of the valve, while in the reference simulation, fluctuations only affected valve 2. On the other hand, valve 2 may be used more often in the implementation than in the reference since it opens at a lower control signal. This could be beneficial since it can prevent valve 2 from getting stuck due to being unused over a longer period of time. Moreover, there is a trade-off between wear on the valves and achieving a fast response resulting in more stable nets. The results presented in Table 6.3 show that the pressure stability was generally improved in the implementation, although the risk of wear on the valves may have increased.

The results indicate that the system responded quicker when valve 2 was restricted to an opening degree of 80%. In the reference where the opening degree of valve 2 varied between approximately 70% and 100%, as seen in Figure 6.2, the corresponding mass flow varied around 4 kg/s in Figure 6.3. In contrast, the opening degree fluctuated around 40% and 80% opening degree in the implementation, resulting in mass flow variations of 10 kg/s. This behaviour can be explained by the valve characteristic, where an opening degree from 80% to 100% does not give any significant mass flow increase. Therefore, it can be desirable to limit the opening degree of the valve to 80% and thus avoid a range with weak response.

7.1.2 Partial Turbine Trip

From the partial turbine trip simulations, the results show no large improvement of the key variables presented in Table 6.2 except for the system losses Q_{loss} which was reduced by just over 8 kWh/h. This reduction means that the pressure relief valves were used to a lesser extent. The fast pressure increase on the 3 bar header increases the inflow into the accumulator, which causes a reduction in the oil usage as the pressure inside the

accumulator increases faster. In the long run, the pressure relief valves are used less since less steam is present in the system.

The pressure stability $\Delta|e(t)|_{MAX}$ was worsened in the 3, 12 and 65 bar headers. The most significant difference is seen in Figure 6.4 which shows the pressure on the 3 bar header, where the implementation model had a larger fluctuation over time. The fast pressure increase may be explained by the fast opening of the reduction valves 65/3 during the overlapping phase, leading to more steam leaving the 65 bar header during a shorter time span. As a consequence, a smaller $\Delta|e(t)|_{MAX}$ is shown on the 65 bar header compared to the reference, which explains the reduction by almost 16% in Table 6.3. Despite the fast response through the reduction valves, the IAE appeared to be worse in the 65 bar header. This can be seen in Figure 6.4, where the controller does not correct the pressure error around 13 060 s - 13 120 s. Since the implementation does not consider re-tuning after the total valve size was changed, that may have impacted the results and the controller's ability to correct for errors.

7.2 Control Hierarchy for 65 Bar Header

From Table 6.4 it is seen that the oil usage increased by almost 1700 kWh/h in the implementation model. This is linked to the deteriorated accumulator usage in the implementation. It is seen in Figure 6.7 and in Appendix A.1 that both the inflow and outflow valves connected to the accumulator were opened simultaneously, causing the accumulator pressure increase rate to be lower in the implementation compared to the reference. This may indicate that the accumulator acts as a bypass between the 65 bar header and the 3 bar header via the 12 bar header, which consequently results in an increased oil fuel input Q_{fuel} as the oil usage is controlled based on the accumulator pressure.

The reason for this bypass behaviour is that the control signal in the 12 bar controller is working in the LL inflow accumulator split block simultaneously as the 3 bar controller is requesting steam from the accumulator. As the 65 bar header experiences steam excess and opens reduction valves 65/12, the 12 bar header closes its turbine extraction valves immediately. Furthermore, the 12 bar header forces the accumulator inlet valve to open by using its LC. As a result, the increased steam flow from the 65 bar header is compensated for, which can be seen in Figure 6.7. It was observed that some of the steam from the 65 bar header, which in the reference model was flowing through reduction valve 65/8, was in the implementation model flowing through reduction valve 65/12 and used to fill the accumulator. As less steam enters the 8 bar header, less steam flows in reduction valve 8/3, which causes the 3 bar header to open the outlet valve from the accumulator, hence the bypass phenomena. In the reference model, both the inflow valve and outflow valve of the accumulator remain closed, which prevents any bypass phenomena from occurring.

By immediately closing the 12 bar turbine extraction valves, the 8 bar header was positively affected as seen from the pressure stability results in Table 6.5. The ΔIAE and $\Delta|e(t)|_{MAX}$ were improved by 38% and 20% respectively. Compared to the reference, the implementation model had a larger steam flow through the turbine to the 8 bar header, which is seen in Figure 6.8. As a result of the increased mass flow from the turbine, the use of reduction valve 65/8 was reduced. This results in the 8 bar header having more

control over its incoming steam flow and can therefore easier maintain its set point pressure level. For the 3 bar header, it was seen that the implementation was improving the pressure stability on that header as well. Since less steam is flowing through reduction valve 65/8, the 8 bar header does not experience steam excess as easily which reduces the use of reduction valve 8/3. As a consequence, the 3 bar header does not experience any steam excess, which explains the decreased steam losses Q_{losses}. Furthermore, the 3 bar header has more control over its incoming steam flow and can thus maintain its pressure level better, which explains the improved pressure stability. In addition, the increased reception of steam from the turbine to the lower pressure levels in the implementation model explains not only the improved pressure stability but also the great increase of electricity generation by 1550 kWh/h since the steam is extracted at a lower pressure.

However, it was observed in the simulation results that the reduction valve 8/3 only was used more at the beginning of the partial turbine trip. When comparing the use of pressure relief valves, seen in Appendix A.2, and the pressure in the 3 bar header over time, lower pressure and more use of pressure relief in the reference model correlate well. Consequently, it can be interpreted as an overcompensation from the 3 bar controller which opens the pressure relief valves more than necessary in the reference model.

It was further observed that the pressure stability on the 12 bar header was greatly improved in the implementation model where ΔIAE and $\Delta|e(t)|_{MAX}$ were improved by 28% and 17% respectively. This can be explained by the weaknesses with extreme feed forward in the system. It is seen in Figure 6.6 that the pressure on the 12 bar header is significantly larger than 12 bar around 13 000 s, achieving almost 12.4 bar in the reference. As the partial turbine trip occurs, steam enters the 8 bar header and followingly the 3 bar header as the 8 bar header experiences steam excess. The first action that the 3 bar controller does to prevent steam excess is, as seen in Figure 5.6a, to open the valve into the accumulator. As a consequence, the 12 bar header receives the information and calls for more steam beforehand to prevent steam deficit. However, the actual steam leaving the 12 bar header was lesser than predicted, resulting in the 12 bar header receiving larger amounts of steam than necessary. This feed forward phenomenon was not noticed in the implementation since steam directly enters the 12 bar header via reduction valves 65/12 instead.

The energy utilisation factor EUF was, seen in Table 6.4, improved by 0.54%. As discussed previously, a trade-off between increased electricity generation and increased oil usage is again observed. In addition, the implementation appears to use the oil fuel input more efficiently as the system losses are reduced, hence the higher value of EUF.

7.3 Control Hierarchy for 3 Bar & 12 Bar Header

This section includes a discussion of the results presented in Section 6.3 during load trip and load start-up, respectively. The implementation appeared to affect the system rather differently in the two operating cases, although the key variables in Table 6.6 had similar tendencies.

7.3.1 Load Trip

The implementation seemed to handle the load trip better when comparing oil consumption, usage of pressure relief valves, and EUF compared to the reference model. Any excess steam in the 3 bar header should yield a faster response in the implementation since a change in the extraction valves from the turbine to the 12 bar header affects the 3 bar header quicker than a change in the accumulator inlet valve. This can be seen in Figure 6.12 where the 3 bar turbine extraction valves are throttled slightly faster in the implementation compared to the reference, which consequently delays the pressure increase at the 3 bar header seen in Figure 6.10. Despite the quicker decrease in mass flow from the turbine extraction valves, the maximum pressure error in the 3 bar header appeared to be slightly larger in the implementation model, and also occurred later compared to the reference model, as seen in Figure 6.10. Since all reduction valves connected to the 3 bar header were closed or used to the same extent in both models, one possible reason why the maximum pressure error is larger can be the decreased use of pressure relief valves in the implementation model.

The pressure stability is observed to be worse in the 12 bar header, as seen in Table 6.7 and Figure 6.10. As the 3 bar header increased the flow from the turbine to the 12 bar header during the load trip, the 12 bar header pressure increased significantly. Consequently, the valve into the accumulator opened faster. When noise is present, it is clear that the 12 bar header experienced more steam excess compared to when no noise is present. The pressure inside the accumulator is initially, and during a long time, lower in the implementation model, which at first sight might seem to contradict the low oil usage. This reduced oil usage is due to the derivative part in the PID-controller that controls the oil usage. It is seen that the pressure inside the accumulator is increasing at a faster pace compared to the reference, which is advantageous for a PID as the derivative part adapts quicker and reduces the oil consumption beforehand. As a consequence of the reduced oil usage, the total amount of steam in the system is reduced, leading to less pressure relief, which explains the great improvement of the reduced steam losses Q_{loss} by just over 780 kWh/h seen in Table 6.6.

Unlike the positive performance factors mentioned above, the electricity generated was noticeably decreased. This is a consequence of reducing the flow through the turbine to the 3 bar header. In addition, it is seen that the reduced electricity production negatively affects EUF as this is considered useful energy.

7.3.2 Load Start-up

The hypothesis of an increased turbine extraction to the 3 bar header in the implementation compared to the reference was unconfirmed in Figure 6.15. In contrast, as the turbine extraction valves to the 12 bar header were closed, the mass flow of steam to the 3 bar header decreased accordingly. Further, it can be seen in Figure 6.15 that the steam extracted from the turbine to the 8 bar header also decreased simultaneously, which indicates that less steam was inserted into the turbine. This was verified in Figure 6.16 as both the turbine insertion from the 110 bar header and the 65 bar header decreased.

The decreased turbine inflow from the 65 bar header can be backtracked to a decreased amount of steam in the header. When the 12 bar turbine outlet valve closed, a steam deficit occurred in the 12 bar header. Therefore, the 12 bar controller opened reduction valve 65/12, as seen in Figure 5.7b. The 65 bar header then experienced a steam deficit and consequently, its controller closed the turbine inlet valve according to Figure 3.4. The controller also reduced the high limit for reduction valves 65/3 to prevent more steam from leaving the header.

As less steam was inserted in the turbine from 65 bar, the 3 bar header received less steam that instead was requested from elsewhere. According to the 3 bar controller split-range in Figure 5.6b, steam should firstly be taken from reduction valves 65/3. However, due to a steam deficit in the 65 bar header, a reduced high limit was set on the reduction valves, restricting the steam flow to the 3 bar header. The 3 bar header was therefore calling for more steam from the 110 bar header via reduction valves 110/3 to satisfy its steam demand. This led to a decrease of steam in the 110 bar header and the 110 bar controller then reduced the mass flow into the turbine. As a result, the issue of less steam extracted from the turbine to the 3 bar header was further amplified since both the 110 bar header and the 65 bar header had a decreased turbine inlet flow. To potentially avoid this issue, a LL of the 12 bar extraction valves could be included in the 12 bar controller. Nevertheless, the system will be more tightly integrated which could lead to an overconstrained system.

An undesired fluctuation can be noticed in the implementation by 22 000 s - 23 000 s in several parts of the system when noise is present. It is seen in an additional simulation, presented in Appendix B.1, that the fluctuations were diminished when the LL 110/3 was altered. The LL 110/3 was then set to zero instead of as in the implementation being determined by the 110 bar controller. This shows that an undesired feed forward issue appeared in the implementation, which also has been noticed in previous studies [19].

Although fluctuations were present in some parts of the system with noise in the implementation, the 8 bar header pressure was more stable, as seen in Table 6.7. When the 12 bar turbine extraction closed, the 8 bar header controlled all the remaining outlet valves from the turbine. Consequently, its steam demand was easier fulfilled and when there was a surplus of steam it was sent further through the turbine to the 3 bar header. Meanwhile, the 12 bar header pressure fluctuated more in the implementation as the turbine outlet valve was closed by the 3 bar header. It can therefore be seen as a trade-off which net that should be prioritised to have stable pressure. The implementation simulations indicate that the pressure stability on the 8 bar header was prioritised, while the reference had less fluctuations in the 12 bar header.

The increased use of reduction valves in the implementation led to a decreased electricity generation from the turbine. At first sight, this could be classed as an impairment of the system as it affects EUF negatively. However, similar to the load start-up in implementation 1, discussed in Section 7.1.1, less electricity was generated from fossil fuels which is preferable.

The decreased oil usage in the implementation is a result of the accumulator pressure being higher. In Appendix B.2, it is seen that the outflow valve from the accumulator opens later in the implementation. This is because the 3 bar controller first closes the 12 bar turbine extraction valves before opening the accumulator outlet. In the reference, where the 3 bar controller first closes its inflow into the accumulator, the accumulator outflow valve opens earlier since the accumulator inflow is already zero. Therefore, the accumulator pressure decreases faster in the reference, seen in Figure 6.14.

Another unexpected result was noticed during load start-up with noise, namely that the oil fuel usage in the recovery boiler was zero both in the implementation and the reference models. Although the accumulator pressure was below the set point value of the boiler, no oil was used. After analysing the different components of the PID-controller connected to the oil usage in the recovery boiler, it was observed that the P-part was mostly positive during load start-up whereas the I-part appeared to be negative, as seen in Appendix B.3. The D-part was small and did not affect the control signal significantly. Consequently, the I-part signal mostly contradicted the P-part signal leading to a negative control signal. The I-part experienced wind-up since it continued to measure the error after the boiler was turned off, wanting to turn off the boiler even further which, in reality, is impossible. As the steam system required more steam later on, the I-part started to increase from its negative value, causing a deadband where no action was taking place.

7.4 Sustainable Development Aspects

Sustainable development can be divided into three parts: ecological, economical and social aspects [23], which all have been considered in this thesis. The United Nations have derived 17 sustainable development goals to strive for [24]. This project is mainly focusing on goals 7-9 listed below:

- 7: Affordable and Clean Energy
- 8: Decent Work and Economic Growth
- 9: Industry, Innovation and Infrastructure

The ecological perspective includes the environmental production capacity, which means that renewable natural resources should be used. Since the thesis has been focusing on decreasing oil usage while retaining the usage of renewable energy, i.e., bark, affordable and clean energy is striven for. The decreased oil usage is also beneficial from an economical perspective, linked to sustainable development goal 8, as fossil fuels are finite natural resources and therefore should be used at minimum and in the most efficient way. In addition, the thesis includes how energy efficiency of the system can be increased. An increased energy efficiency can lead to an increased profit in terms of monetary capital.

Without a control system, operators need to manually control the steam net. The system is presumably more efficient when automatic control is applied compared to being manually controlled from operators. For instance, the control system is likely to take action

quicker by opening or closing valves when a steam deficit or surplus occurs as the delay of a human to react is avoided. Automatic control can not only be linked to sustainable development goals 7 and 8, but also contributes to achieve sustainable development goal 9 as development of the control system is a part of industrialisation and innovation. Additionally, a control system is to be preferred over operators due to the high complexity of the system and high pressure levels, which creates a dangerous environment with high risks to work in. A dangerous working environment can therefore be avoided, which can be coupled to the social aspect of sustainable development.

8

Conclusion

In the first implementation where non-linearity and an overlapping opening sequence were added, the control of reduction valves was modified. The implementation indicated that non-linear valves generally generate more fluctuations in the steam system compared to when all valves are assumed to be linear. With the tested valve characteristic, an overlap of the opening degree for the two 65/3 reduction valves gave a quicker response, resulting in an improved system stability compared to when serial opening was applied. Moreover, by restricting the opening degree of valve 2 to 80%, a deadband with a weaker response was removed. However, each individual case needs to be considered if an overlapping opening sequence shall be implemented in a system depending on the characteristics of the valves. Lastly, no significant improvement in energy efficiency was observed in the implementation, as EUF was not majorly affected. Nevertheless, the implementation used less oil, as desired, but as a trade-off, less electricity was generated.

From the results of the second implementation with the added LL 65/12, it can be concluded that the system stability was increased or maintained in all pressure headers during the partial turbine trip. Similar to the first implementation, a trade-off between increased electricity generation and oil fuel input was observed. The system appeared to work more efficiently with its fuel input as the steam losses were reduced and EUF increased. Furthermore, this control hierarchy did not result in a more efficient usage of the accumulator since it functioned as a bypass between the headers, which is not desirable. However, if pressure stability is prioritised over using the accumulator more efficiently, this implementation is recommended.

The development of the control hierarchy was also concerned in the third implementation, in which the control of the accumulator inflow valve and the turbine extraction at 12 bar were altered. The EUF increased during the load trip but decreased slightly during load start-up. In both cases, oil usage was decreased, as desired, since the accumulator was filled faster during the trip and emptied slower during start-up. Thus, the accumulator was used more efficiently in this implementation. Due to the decreased fuel usage, the electricity generation and steam losses decreased in both cases. The new control of the turbine did not increase the steam flow to the 3 bar header as firstly assumed, and the stability was generally deteriorated, except for the 8 bar header during load start-up which showed a large pressure stability improvement. It can therefore be concluded that there is a trade-off between efficient use of the accumulator and system stability.

9

Future Work

This thesis has been based on simulations for chosen scenarios where the system stability and the effects of the implementations on the system were assessed. However, to fully evaluate whether the implementations are improving or deteriorating the system, more cases can be tested. For instance, it would be insightful to investigate how well the system responds to a total turbine shutdown, which can happen during, e.g., maintenance. Also, load trips and load start-ups on other nets than the 3 bar header can be simulated to get a better picture of the system robustness. Other scenarios that can be tested to get an insight into the characteristics of the pulp and paperboard mill are different types of noise. These are variations that have been outside the scope of this thesis, yet it is disturbances that the system shall be robust enough to handle.

For further development of the model, a combination of the implementations can be simulated. In this thesis, the simulations have included each implementation separately to validate how the system responds to each change. However, if all implementations are included in the same model they may yield larger effects. For example, by combining implementation 2 and implementation 3 the hierarchy is changed in the 65 bar, 12 bar, and 3 bar headers. This may result in an even more stable pressure on the 12 bar header as the header controller has more control handles.

The current system is restricted to only using oil, bark, and black liquor as fuel input. As society is heading towards minimising the use of fossil fuels, an interesting evaluation would be to diminish the oil usage in the system. However, both bark and black liquor give a slow response to fluctuations, and it is therefore necessary to have a fuel that can respond quickly to changes. A potential replacement for oil can be biofuels, such as using a fluidised bed or biogas. Further investigations are then needed regarding how well this change may respond to fluctuations, as well as determine the feasibility of replacing oil with biofuel.

Since only a Dymola model of the pulp mill has been used to evaluate the implementations, several simplifications have been made. Tests have only been done on a model including two non-linear valves with one type of valve characteristic in the first implementation. If tests can be performed to determine real valve characteristics of other valves, this can be included to get a more realistic model of the system today. Other investigations can be done on the real model and then included in the Dymola model, e.g., how much the pressure relief valves are allowed to be used and what stability requirements each pressure

level has to meet the process steam demand.

To receive more accurate results, the controllers that were affected by the implementations need to be re-tuned. Controllers are tuned for a specific system, and due to the modifications that have been made, the values of the controller parameters need to be reconsidered to truly assess the impact of the implementations and to better evaluate the modified control system. Furthermore, by re-tuning the controllers it is easier to discern whether pressure errors are due to the implementation or the selected parameters of the controllers.

An economic evaluation has been excluded, as it is outside the objective. However, it might be valuable to determine potential cost savings when the implementations are used during different operating stages and electricity prices. It may be desired to e.g., increase the fuel usage to provide the system with electricity when the electricity prices are high.

9.1 Suggestions

The following section contains a summarised list of recommended future work:

- Model and simulate a combination of the implementations.
- Investigate different fuel types in the system, such as biofuels.
- Identify realistic valve characteristics for each valve in the steam system.
- Investigate the boundaries of the existing system and add them to the Dymola model, e.g., maximum allowable usage of pressure relief valves and stability requirements on each pressure level.
- Tune the controllers in the steam system for each implementation.
- Perform economic evaluations of the implementations.

Furthermore, the following list contains operating cases that might be of interest to better understand the system:

- A turbine trip.
- A planned turbine shutdown.
- A turbine start-up.
- Load trips on all consumer headers.
- Load start-ups on all consumer headers.

Bibliography

[1] *Solvina AB*. Date of access: 2024-06-04. URL: https://www.solvina.com/.

[2] *Skogsindustrierna*. Date of access: 2024-04-06. URL: https://www.skogsindustrierna.se/om-oss/medlemmar/karta/.

[3] International Energy Agency. *Emissions from Oil and Gas Operations in Net Zero Transitions A World Energy Outlook Special Report on the Oil and Gas Industry and COP28*. Tech. rep. Date of access: 2024-04-15. URL: www.iea.org.

[4] The Physics Classroom. *What Does Heat Do?* Date of access: 2024-06-04. URL: https://www.physicsclassroom.com/class/thermalP/Lesson-2/What-Does-Heat-Do.

[5] Nikolai V Khartchenko and Vadym M Kharchenko. *Advanced Energy Systems*. 2nd ed. Energy Technology Series. CRC Press LLC, 2013. ISBN: 9781482216882.

[6] The Engineering Toolbox. *Fuels - Higher and Lower Calorific Values*. Date of access: 2024-03-20. URL: https://www.engineeringtoolbox.com/fuels-higher-calorific-values-d_169.html.

[7] Klaas Jan Kramer et al. "Energy efficiency improvement and cost saving opportunities for the pulp and paper industry". In: *Berkeley, CA: Lawrence Berkeley National Laboratory* (2009).

[8] Tadashi Tanuma. *Advances in Steam Turbines for Modern Power Plants*. English. Woodhead Publishing Series in Energy. [S.l.]: Woodhead Publishing, 2022. ISBN: 9780128243596. DOI: https://doi.org/10.1016/C2020-0-01671-3.

[9] Jan Votava et al. "Optimized Use of the Steam Accumulator in the Combined Heat and Power Production". In: *2019 20th International Scientific Conference on Electric Power Engineering (EPE), Electric Power Engineering (EPE), 2019 20th International Scientific Conference on*. IEEE, May 2019, pp. 1–5. ISBN: 978-1-7281-1334-0. DOI: 10.1109/EPE.2019.8778141.

[10] Philip L. Skousen. *Valve Handbook*. 3rd Edition. McGraw-Hill's AccessEngineering. McGraw-Hill Education, 2012. ISBN: 9780071743891. URL: https://www.accessengineeringlibrary.com/content/book/9780071743891.

[11] Spirax Sarco. *Basic Desuperheater Types*. Date of access: 2024-05-16. URL: https://www.spiraxsarco.com/learn-about-steam/desuperheating/basic-desuperheater-types?sc_lang=en-GB.

[12] Tore Hägglund. *Praktisk processreglering*. 4:1. Studentlitteratur AB, 2019.

[13] Brian Nesbitt. *Handbook of Valves and Actuators*. 1st ed. Elsevier Science & Technology, June 2007. ISBN: 9781493303885.

[14] NextPCB. *What is an Actuator? Types, Principles, and Applications*. Date of access: 2024-06-04. URL: https://www.nextpcb.com/blog/What-is-an-actuator-types-principles-and-applications.

[15] Curtis D. Johnson. *Process control instrumentation technology*. 3rd ed. John Wiley & Sons, Inc., 1988.

[16] Karl J Åström and Tore Hägglund. *Advanced PID Control*. International Society of Automation (ISA), 2006. ISBN: 978-1-55617-942-6.

[17] Krister Forsman. *Reglerteknik för processindustrin*. 1st ed. Studentlitteratur, 2005. ISBN: 9789144037899.

[18] Eskil Svensson. *Evaluation of Smart Split-Range Control Strategies for Optimized Turbine and Steam Control in Pulp and Paper Plants*. Tech. rep. Luleå Tekniska Universitetet, 2019.

[19] Pontus Svensson. *Evaluation of a decentralized control system for steam-networks*. Tech. rep. Göteborg: Chalmers Tekniska Högskola, 2020.

[20] Rebio AB. *Sågverksbränske*. Date of access: 2024-0-06. URL: https://www.rebio.se/vara-produkter/sagverksbransle/.

[21] Pratima Bajpai. "Pulping Fundamentals". In: *Biermanns' Handbook of Pulp and Paper*. Vol. 1. Elsevier, 2018. Chap. 12, pp. 295–351. DOI: https://doi.org/10.1016/B978-0-12-814240-0.00012-4. URL: https://www.sciencedirect.com/science/article/pii/B9780128142400000124.

[22] Tore Hägglund. "Industrial implementation of on-line performance monitoring tools". In: *Control Engineering Practice* 13.11 (Nov. 2005), pp. 1383–1390. ISSN: 09670661. DOI: 10.1016/j.conengprac.2004.12.006.

[23] Fredrik Hedenus, Martin Persson, and Frances Sprei. *Sustainable Development - Nuances and Perspectives*. 2nd ed. Studentlitteratur AB, 2022. ISBN: 9789144161150.

[24] The United Nations. *The 17 Goals*. Date of access: 2024-06-04. URL: https://sdgs.un.org/goals.

A

Control Hierarchy for 65 Bar Header

The figures presented in this chapter are further discussed in Chapter 7.2.

A.1 Accumulator Outflow Valve

In Figure A.1 the mass flow and opening degree of the accumulator outflow valve are presented. During partial turbine trip, the valve opened more in the implementation, causing a bypass phenomenon in the accumulator.

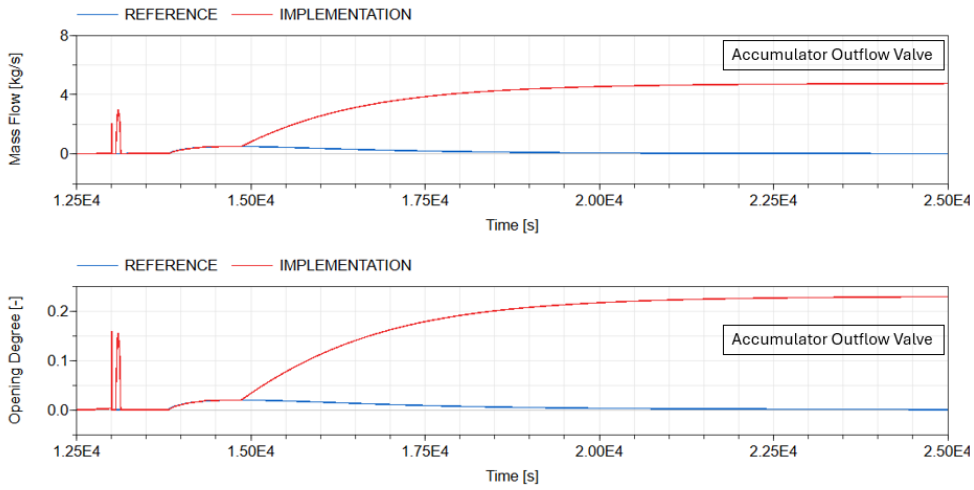

Figure A.1: Mass flow and opening degree of the accumulator outflow valve.

A.2 Pressure Relief Valves

The mass flow in the pressure relief valves during partial turbine trip is plotted in Figure A.2. It can be seen that the pressure relief valves were used less in the implementation where LL 65/12 has been added to the 65 bar header's controller compared to the reference.

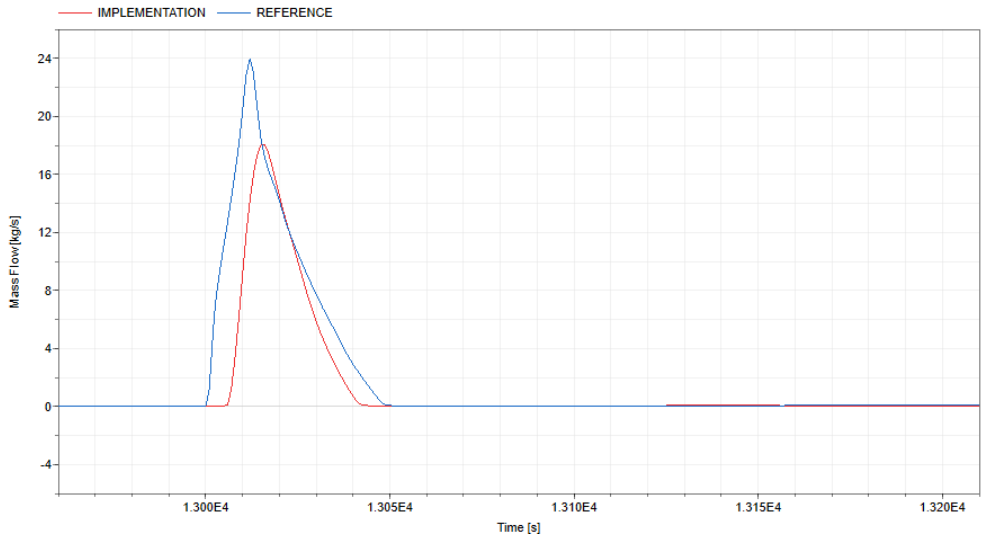

Figure A.2: Mass flow in pressure relief valves during partial turbine trip.

B

Control Hierarchy for 3 Bar & 12 Bar Header

The figures presented in the following sections are further examined in Section 7.3.2.

B.1 Fluctuations in the System

In Figure B.1, graphs from the fluctuation test are presented during load start-up for the implementation where the control hierarchy for the 3 bar and 12 bar header was modified. The fluctuation test included a comparison between the implementation found in Chapter 6.3 with a LL on valve 110/3 and a simulation without a LL on valve 110/3. It can be seen that the fluctuations were reduced in valve 110/3, 65/3 and turbine insertion at 110 bar when the LL 110/3 was removed.

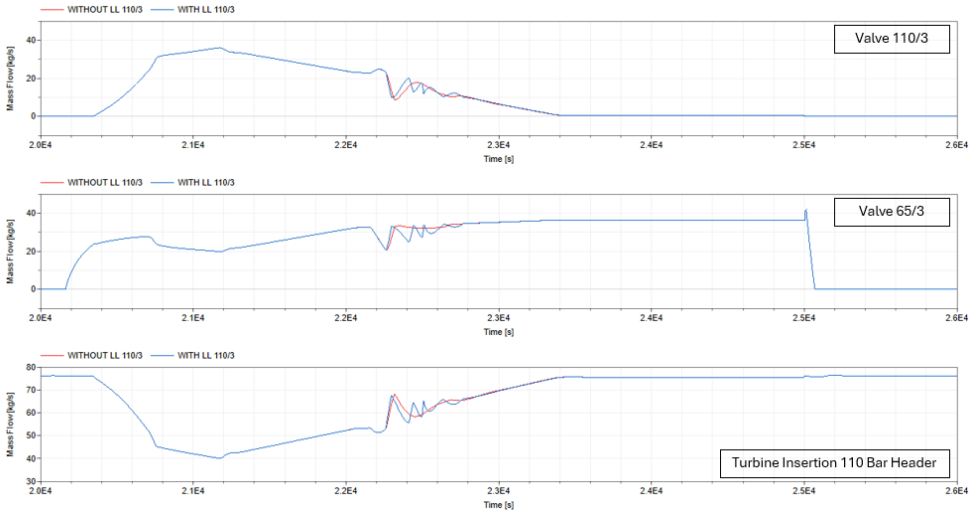

Figure B.1: Mass Flow through valve 110/3, 65/3 and turbine insertion at 110 bar.

B.2 Accumulator Outflow Valve

Figure B.2 shows the mass flow and opening degree of the accumulator outflow valve to the 3 bar header during load start-up. As seen, the valve opens later in the implementation compared to the reference.

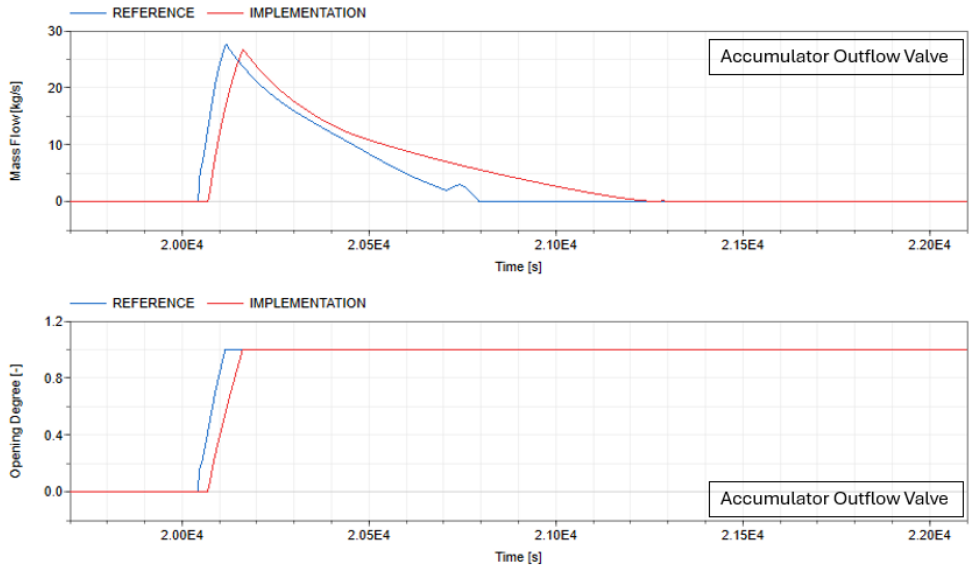

Figure B.2: Mass Flow and Opening Degree of the accumulator outflow valve during load start-up.

B.3 Windup Phenomena

As shown in Figure B.3, a windup phenomena appeared both in the reference and the simulation during load start-up.

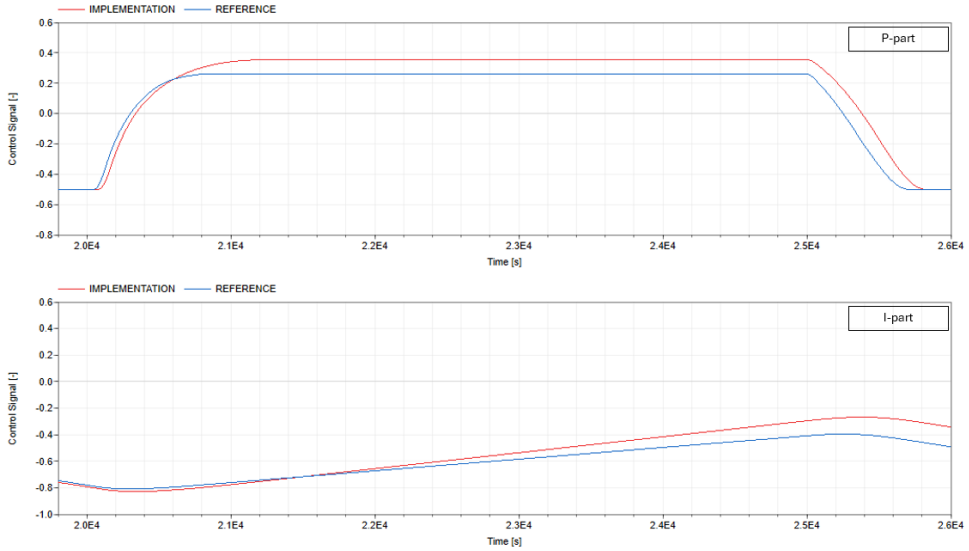

Figure B.3: P-part and I-part of the controller that is regulating oil usage in the recovery boiler.

DEPARTMENT OF ELECTRICAL ENGINEERING
CHALMERS UNIVERSITY OF TECHNOLOGY
Gothenburg, Sweden
www.chalmers.se

CHALMERS
UNIVERSITY OF TECHNOLOGY